

Mohr's Circle and more circles

Rebecca Brannon

Warning: this document is rather rough. I wrote it as a self-study guide for students who wanted a refresher on Mohr's circle and for more advanced students who are ready to learn about extending Mohr's circle to non-symmetric matrices (and to see Mohr's circle be used for something more interesting than simple coordinate transformations).

Mohr's circle was extremely popular in its day, so the vast majority of these results are not new -- it is baffling our community continues to publish papers about Mohr's circle to "report" information that was known even in the early 1900s!

ABSTRACT

Traditionally, Mohr's circle has been used as a graphical method for performing coordinate transformations for stress, but the technique applies equally well to *any* 2×2 tensor matrix. Mohr's circle also provides rapid graphical estimations for eigenvalues and eigenvectors, which is extremely useful for verifying analytical results. Mohr's circle is *not* just for stress tensors, but it is typically taught in only that context in introductory materials mechanics courses. For stress tensors, Mohr's circle can be used to visualize and to determine graphically the normal and shear stresses acting on a plane of any given orientation. For symmetric tensors, Mohr's circle can be generalized to 3×3 matrices for a graphical depiction of the set of all possible normal and shear components. The traditional definition of Mohr's circle for symmetric matrices is presented with numerous examples for performing coordinate transformations, finding the plane(s) of maximum shear, and identifying eigenvalues and eigenvectors. An important but little-known enhancement to Mohr's circle (called the Pole Point) is shown to rectify counter-intuitive factors of 2 when converting angles in physical space to angles in the Mohr diagram. The extension of Mohr's circle to 3×3 matrices is presented with application to the Mohr-Coulomb theory of material failure. The basic construction of Mohr's circle is shown to apply with only minor modification to nonsymmetric matrices, in which case the circle no longer remains symmetric about the normal axis. Applications of nonsymmetric Mohr's circle include rapid eigenvalue/eigenvector determination and fast polar decompositions for deformation matrices. A numerical exploration is presented that suggests there is no simple extension of Mohr's circle to 3×3 nonsymmetric matrices.

1. Introduction

In a first course on mechanics of materials, you were probably introduced to the application of Mohr's circle to perform coordinate transformations on two-dimensional stress states, but did you ever look at it closer? Mohr's circle is more than just a tool to analyze *stress*. It can be applied to any 2×2 symmetric matrix, such as strain or moments of inertia. As a matter of fact, the matrix doesn't even have to be symmetric!

Mohr's circle does nothing that you can't do using purely analytical methods, so why is it useful? Mohr's circle is extremely valuable as a quick graphical estimation tool to double-check your analytical work. As shown in Section 2, you can use it to determine eigenvalues of a matrix or to estimate the orientation of a reference frame in which the shear stresses are maximized. More recently, as depicted in Fig. 1.1, Mohr's circle has been "re-discovered" for visualizing tensor fields. The upper part of that figure shows a spherical salt body embedded in a large expanse of rock. The overburden at a point (i.e., the weight of rock above) increases linearly with depth. Unlike fluids, solids (like rock) can have both normal and shear stresses (maximum shearing, in this problem, occurs on planes 45° off-vertical). The small diagram at the bottom of Fig. 1.1 (called a Mohr diagram) shows a collection of circles that are cross-matched in color to the computational domain. The horizontal axis represents normal stresses and the vertical axis represents shear stresses. At any given location in space, the normal and shear stresses depend on the plane on which they act. For example, there are no shear stresses on horizontal planes (except near the salt body). On the other hand, shear stresses do act on differently oriented planes. Otto Mohr proved that the set of all possible shear-normal stress pairs acting on planes of various orientations at a point will always fall within or on a circle (Mohr's circle). As you move deeper below the rock surface, the circles translate to the left (indicating increasing levels of compressive — negative — stress). The circles also increase in radius (indicating increasing levels of shearing). The "bumps" you see in the profile indicate how much the presence of the salt sphere perturbs the lithostatic stress field.

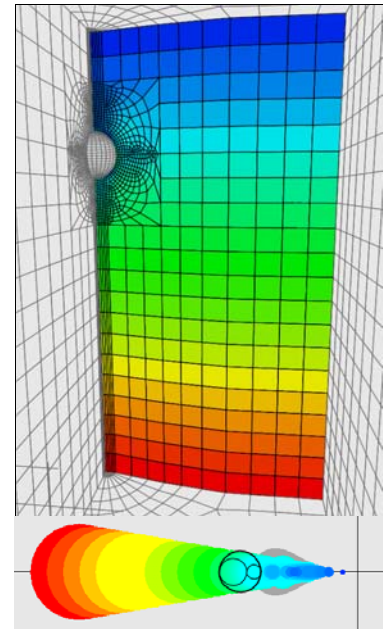


Figure 1.1. Application of Mohr's circle to visualization of a spatially varying stress field. Ref: Crossno, Rogers, and Brannon (2003).

In this tutorial, we will review the basic instructions for constructing and interpreting Mohr's circles. Those who already know Mohr's circle may recall that an angle gets doubled when portrayed in Mohr's circle, which can be very confusing. Section 2 introduces a little known enhancement to Mohr's circle (namely, the Pole Point) that rectifies this problem. Some engineering applications of the 2D Mohr's circle are provided.

As shown in Section 3, you can generalize Mohr's circle for *nonsymmetric* 2×2 matrices. With the nonsymmetric Mohr's circle, you can graphically determine whether there are real eigenvalues and whether the algebraic multiplicity of an eigenvalue equals its geometric multiplicity, and you can graphically determine right and left eigenvectors. When the nonsymmetric Mohr's circle is applied to the deformation gradient tensor from continuum mechanics, you can quickly determine the polar decomposition rotation and stretch.

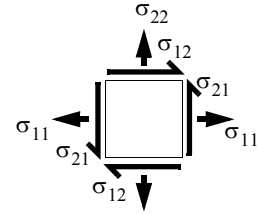
In the trailing part of Section 2 we will review how Mohr's circle generalizes for 3×3 symmetric matrices. The trailing part of Section 3 also explores whether there exists a similar generalization for *non-symmetric* 3×3 matrices. A clear generalization from 2D to 3D Mohr diagrams in this case of nonsymmetric tensors is not readily apparent. However, some publications have been recently brought to our attention that purport to address this problem, so look back at this tutorial at a later date to see if we have any more news on that front.

What is Mohr's circle?

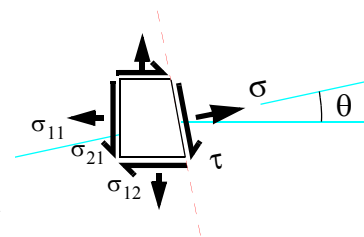
Suppose that you know the components of a 2D stress matrix,

$$\begin{bmatrix} \sigma_{11} & \sigma_{12} \\ \sigma_{21} & \sigma_{22} \end{bmatrix}. \quad (1.1)$$

These components are referenced to some particular basis — probably the fixed laboratory basis $\{\underline{E}_1, \underline{E}_2\}$. If you look at the same stress state from some other orientation, then the components will be different. The formula for the reoriented stress components is given in the Appendix, but the formula is awkward and lacks physical or mnemonic insight. Otto Mohr (1835-1918) developed Mohr's circle as an *easily-remembered* technique to *graphically* determine new stress components with respect to any rotated basis.*



The fundamental idea behind Mohr's circle is that the normal and shear stresses on a plane depend on the orientation of that plane. Suppose that we slice the above stress element with a plane whose outward normal makes an angle θ with the horizontal. There are two values of θ (namely, 0 and $\pi/2$) where we already know the normal and shear stress. Consider the orientation where the plane's outward normal is parallel to the \underline{E}_1 laboratory base vector; in other words, suppose that $\theta=0$. Then comparing the above two sketches, we know that the normal stress σ must equal σ_{11} and the shear stress τ must equal $-\sigma_{21}$. There's a negative sign because we arbitrarily decided to show τ such that it tended to shear the stress element in a clockwise direction, but the first figure shows σ_{21} in the opposite direction. As the orientation of the plane is varied, the normal and shear stresses will vary smoothly until eventually $\theta=\pi/2$. At this orientation, the outward normal of the cutting plane will be aligned with \underline{E}_2 and a comparison of the above two drawings shows that $\sigma = \sigma_{22}$ and $\tau=+\sigma_{12}$ when $\theta=\pi/2$.



Noting that τ and σ are functions of θ , we can imagine parametrically plotting τ vs. σ for various values of θ . It is proved in the Appendix that the resulting plot will always turn out to be a circle — Mohr's circle. We will show that moving by an amount $\Delta\theta$ in the physical plane will correspond to moving an angular distance $2\Delta\theta$ on Mohr's circle. Consequently, Mohr's circle may be used to perform coordinate transformations. For symmetric matrices such as stress, Mohr's circle will always be centered about the σ -axis. For nonsymmetric matrices, it will lie off the σ -axis. Now let's cover these concepts in greater detail.

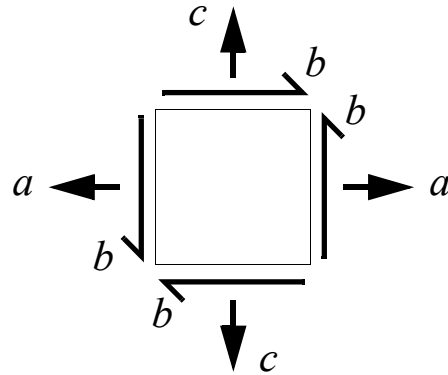
* Original work: Mohr, O. (1900) Welche Umstaumlaut **Finish citation from Jaeger and Cook Rock Mechanics book (mohr 1900 and~1915)**

2. Mohr's Circle for symmetric matrices

Consider a generic 2×2 symmetric matrix:

$$\begin{bmatrix} a & b \\ b & c \end{bmatrix}. \tag{2.1}$$

This does not have to correspond to a stress state, but, for constructing Mohr's circle, it is nevertheless useful to "pretend" that the matrix is a stress state where $\sigma_{11} = a$, $\sigma_{12} = \sigma_{21} = b$, and $\sigma_{22} = c$. This stress state is sketched at right.



To construct Mohr's circle, you examine the normal and shear stresses on each face to construct a pair of numbers for each face.

The face whose outward unit normal is horizontal will be called the "H" face and the face whose outward normal is vertical will be called the "V" face. For the stress state shown above, the normal stress on the H-face equals a , and the normal stress on the V-face equals c . The normal stress is considered positive if it is in tension, and negative if it is in compression.

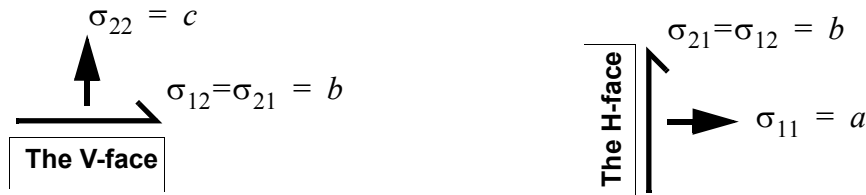
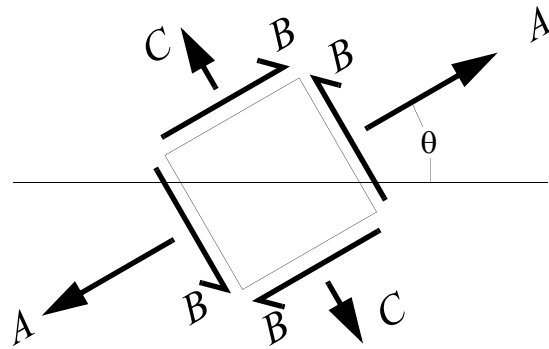


Figure 2.1. The H and V faces of the "stress" element. The outward normal of the H face is horizontal and the outward normal of the V face is vertical.

For the purpose of Mohr's circle, the shearing stress *on a face* will be given a numerical sign according to a *left-hand rule*. In other words, the shearing stress on a face is positive if it tends to torque the stress element in the *clockwise* direction. The shearing stress is negative if it torques the stress element in the counter-clockwise direction. Thus, the shearing stress on the H-face equals $-b$ while the shearing stress on the V-face equals $+b$. For symmetric matrices, the shearing stresses on the two faces always "balance" each other so that there is no net torque. Later on, when we discuss non-symmetric matrices, the torques will *not* balance, but we will find that most of the discussion covered here for symmetric matrices also holds true for nonsymmetric matrices. The reason for the left-hand rule will become apparent later. Many authors* use a right-hand rule, which might feel more familiar to some, but precludes several extremely appealing properties of Mohr's circle (especially the pole point). The direction of shearing is only a *choice*, and you can convert from one convention to another by merely changing a sign. In a loose

sense, a counter-clockwise (right-handed) rotation of a stress tensor itself (holding your own orientation fixed) is equivalent to a clockwise (left-handed) rotation of yourself (leaving the stress element untouched), so the issue of sign conventions for rotations will always be there, no matter what route you take. With our left-handed convention, the key thing that you need to remember is that the stress *matrix* will always use a convention for which a positive off-diagonal component corresponds to a counterclockwise shear on the 1-face and, to balance torques, a clockwise shear on the 2-face.

For coordinate transformations, we desire to know what the normal and shear stresses would be for a stress element that is oriented at some known angle θ to our stress element (see figure). Recalling that the shearing stress is positive on one face and negative on the other, it stands to reason that the shearing stress must transition smoothly from one sign to the other, so there exists a special element orientation (the principal orientation) for which the shearing stress is zero. A common engineering problem involves determining this special shear-free orientation. This task is tantamount to doing an eigenvalue analysis on the original stress matrix. For boundary value problems, we might need to know the traction (*i.e.*, the normal and shear stresses) exerted on a surface of known orientation. Mohr's circle is helpful for all these practical applications.



If we find a method for determining the normal and shear stresses on a face whose normal makes an angle θ with the horizontal, then we have also found a means of determining the normal and shear stresses on the other faces. In the above figure, the face whose normal stress is C is at angle $\theta + \pi/2$, so we can just apply our formulas using this angle to obtain the shearing and normal stresses on that face.

* For example,
Nutbourne & Martin (1988, p171), **Differential Geometry**. Addison-Wesley, Reading, MA.
Reismann, H. & Pawlik, P.S. (1980), **Elasticity: Theory and Applications**, Krieger Publishing Co., Malabar, FL

Mohr diagram

We seek a method of computing the normal and shear stresses on a plane whose normal makes an angle θ with the horizontal. These shearing and normal stresses depend on the orientation of the plane. On any given plane, we will say that the normal stress σ is positive if it is tensile. We will say that the shearing stress τ is positive if it tends to rotate the face in a *clockwise* direction. In other words, the numerical sign for the shearing stress is assigned by using a *left-hand rule*. Although it is not obvious now, a left-hand rule is adopted in order to make certain properties of Mohr's circle more appealing.

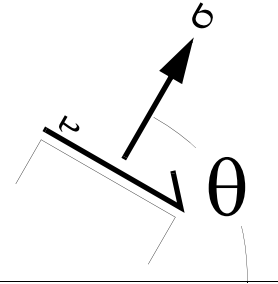


Figure 2.2. Sign convention for normal and shearing "stress" on a plane.

Recall that the normal and shearing stresses depend on the orientation of the plane. They must transition smoothly from their values on the H-face to those on the V-face. Comparing Fig. 2.2 with Fig. 2.1, we observe that

$$\begin{aligned} \text{On the H-face } (\theta = 0): \quad & \sigma = \sigma_{11} = a \quad \text{and} \quad \tau = -\sigma_{21} = -b. \\ \text{On the V-face } (\theta = \frac{\pi}{2}): \quad & \sigma = \sigma_{22} = c \quad \text{and} \quad \tau = +\sigma_{12} = +b. \end{aligned} \quad (2.2)$$

Henceforth, we will make such statements more compactly by simply writing the ordered pairs (normal stress, shearing stress) for each face:

$$\begin{aligned} \text{H: } & (a, -b) \\ \text{V: } & (c, b) \end{aligned} \quad (2.3)$$

The value of τ on the H-face is negative of the value of τ on the V-face. This property always holds for symmetric matrices — the shearing stresses must balance. Of course, you can always forego drawing a stress element by directly noting the correspondence:

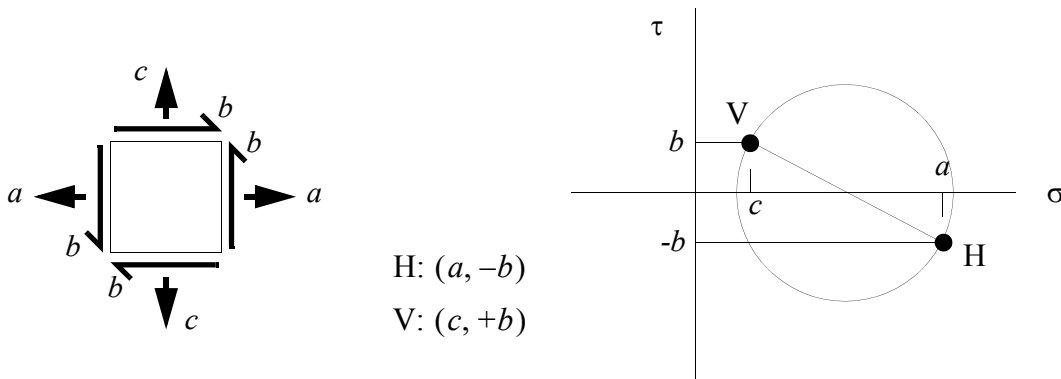
$$\begin{bmatrix} a & b \\ b & c \end{bmatrix} = \begin{bmatrix} H_1 & V_2 \\ -H_2 & V_1 \end{bmatrix}. \quad (2.4)$$

We are interested in the values of σ and τ on a plane of arbitrary orientation θ . These quantities vary with θ . We can imagine a graph in which the smoothly varying shearing stress $\tau(\theta)$ is plotted parametrically against the corresponding normal stress $\sigma(\theta)$ for various values of the orientation angle θ . Naturally the points on such a graph must begin repeating themselves (due to periodicity of the angle θ). Hence, we expect the family of (σ, τ) points to form some sort of closed path in the τ vs. σ space. It is proved in the Appendix that this closed path will in fact be a *circle*, which is called Mohr's circle.

The H-face corresponds to $\theta=0$. Hence Eq. (2.3) tells us that Mohr's circle must pass through the H-point $(a, -b)$. It must also pass through the V-point (c, b) when $\theta=\pi/2$. Consequently, we have deduced two points that must lie on the circle. Ordinarily, it takes three points to uniquely define a circle, but the Appendix provides a proof of the following very important property of any Mohr's circle:

Whenever the orientations of two planes differ by exactly 90 degrees, the corresponding points on Mohr's circle will be diametrically opposite each other.

Consequently, not only are the H and V points from Eq. (2.3) located somewhere on Mohr's circle, they are also on *opposite sides* of Mohr's circle! This added restriction uniquely defines the Mohr's circle. To construct Mohr's circle, simply plot H and V, and then draw a circle such that the line connecting H and V is a major diameter of the circle (see figure).



Keep in mind: Mohr's circle is a parametric plot of the shear and normal stresses on a plane as a function of the plane's orientation angle θ . Thus, when you read the (σ, τ) coordinates of a particular point on Mohr's circle, then you know that *there exists* a plane on which the normal and shear tractions are given by those values. At this point, *you do not know the orientation of the plane*. Later on, we will show that the orientation of the plane is exactly half of the angular distance from the H-point on the Mohr's circle to the (σ, τ) point of interest. For now, let's focus on how to draw Mohr's circle and how to draw general conclusions from the Mohr's circle.

EXAMPLE 1. Use Mohr's circle to quickly decide if the following matrix has any negative eigenvalues.

$$\begin{bmatrix} 1 & -2 \\ -2 & 3 \end{bmatrix}. \tag{2.5}$$

SOLUTION: First, please note that Mohr's circle is not the easiest way to answer this question. You can simply check the signs of the invariants. The first invariant is

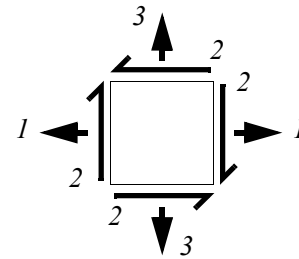
$$\text{trace} = \text{sum of diagonals} = 1 + 3 = 3. \tag{2.6}$$

The second invariant is

$$\text{determinant} = (1)(3) - (-2)(-2) = -1. \tag{2.7}$$

The invariants are not *both* positive, so the matrix does indeed have at least one negative eigenvalue. Now, for the purpose of illustration, let's solve the problem using Mohr's circle.

Imagine that this matrix represents a "stress element" as shown here. The shearing stress is labeled as "2" instead of "-2" because the negative sign is already reflected accurately in the drawing. The question now becomes: Does this stress element have any plane on which the normal stress is compressive?



To answer this question, first we construct the Mohr's circle. Consider the face with a horizontal normal. The normal stress on this H-face is 1, and the *left-hand rule* says the shearing stress on the H-face equals +2. Hence, the H-point on Mohr's circle is (1,2). On the face with a vertical normal, the normal stress is 3, and (again by the left-hand rule) the shearing stress is -2. Thus we have our two points that define the Mohr's circle. Namely

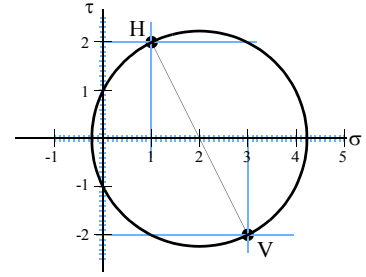
$$\begin{aligned} \text{H: } & (1,2) \\ \text{V: } & (3,-2). \end{aligned} \tag{2.8}$$

An alternative way to obtain the H and V points is to apply Eq. (2.4). Namely, we write

$$\begin{bmatrix} 1 & -2 \\ -2 & 3 \end{bmatrix} = \begin{bmatrix} H_1 & V_2 \\ -H_2 & V_1 \end{bmatrix}, \tag{2.9}$$

from which we directly note that $H_1=1$, $H_2=2$, $V_1=3$, and $V_2=-2$, in agreement with Eq. (2.8).

We must plot the H and V points in τ vs. σ space, and draw a circle such that the line connecting H and V is a major diameter. The final result is shown at right.



Getting back to the original question, we want to know if there are any planes on which the normal stress σ is compressive. Recall that points on the Mohr's circle correspond to the normal and shear stresses on planes of various orientations. Noting that this circle does indeed have some

points where $\sigma < 0$, we conclude that there do exist planes on which the normal stress is compressive. Therefore, the original matrix of Eq. (2.5) does have a negative eigenvalue.

As a matter of fact, the eigenvalues are identically equal to the two values of σ where $\tau=0$. Let C_M denote the value of σ at the *center* of Mohr's circle. Let R_M denote the radius of Mohr's circle. Inspecting the geometry of the circle, we see that the circle is centered at $C_M = 2$ and the circle's radius is $R_M = \sqrt{2^2 + 1^2} = \sqrt{5}$. Hence the two eigenvalues of the matrix in Eq. (2.5) are

$$C_M \pm R_M = 2 \pm \sqrt{5}. \quad (2.10)$$

Notice that we were able to assert the existence of at least one plane on which the normal stress was compressive, and we did this without having to *find* the actual orientation of a suitable plane. It will soon be shown that Mohr's circle may also be used to find the orientations of planes with desired properties (or, conversely, to find the stresses on a plane of known orientation). For now, however, let's focus on further practice with constructing Mohr's circle.

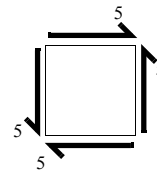
Exercise 1. Demonstrate graphically (*i.e.*, by accurate drawings, not by using trigonometry) that the Mohr's circles for *all* of the following matrices are identical to the Mohr's circle in Example 1. The key (and *only*) distinguishing feature is the location of the H (and V) point. Marking the H and V points will later be crucial for you to interpret a Mohr's circle. The H and V points tell you the connection between the stress element and its orientation relative to the laboratory coordinates.

$$\begin{bmatrix} 1 & 2 \\ 2 & 3 \end{bmatrix} \quad \begin{bmatrix} 3 & 2 \\ 2 & 1 \end{bmatrix} \quad \begin{bmatrix} 3 & -2 \\ -2 & 1 \end{bmatrix} \quad \begin{bmatrix} 0.13 & 1.23 \\ 1.23 & 3.87 \end{bmatrix} \quad \begin{bmatrix} 2+\sqrt{5} & 0 \\ 0 & 2-\sqrt{5} \end{bmatrix}. \quad (2.11)$$

EXAMPLE 2. The following matrix and stress element correspond to pure shear of magnitude 5:

$$\begin{bmatrix} 0 & 5 \\ 5 & 0 \end{bmatrix}.$$

(2.12)



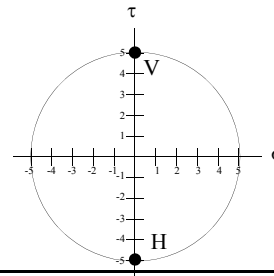
Referring to the stress element (remembering to apply the *left-hand rule* for shearing stresses), the H and V points are

H: (0, -5)

V: (0, 5).

(2.13)

The corresponding Mohr's circle is shown at right. For pure shear, the Mohr's circle will always be centered at the origin. Conversely, if the Mohr's circle is centered at the origin, then the stress element is in a state of pure shear. The matrix of Eq. (2.12) is fairly obviously in a state of pure shear, but Exercise 2 shows that the same stress state might *appear* radically different when viewed from some other perspective.



Exercise 2. Show that the following matrix corresponds to a state of pure shear that is identical to that of Example 2; the only difference is the locations of the H and V points. In other words, this matrix corresponds to the *same* stress state as seen by a differently-oriented observer.

$$\begin{bmatrix} -4 & 3 \\ 3 & 4 \end{bmatrix}.$$

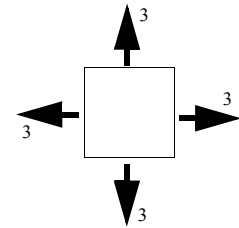
(2.14)

Exercise 3. Construct a matrix that corresponds to the same stress state as in Eqs. (2.12) and (2.14) except as seen from a perspective in which there are no shearing tractions on the H and V planes. What are the eigenvalues of the matrices in Eqs. (2.12) and (2.14)? How do these eigenvalues compare to those of the matrix that you just constructed?

Hint: locate the only two points on the Mohr's circle where $\tau=0$. Take the H-point to be one of these and the V-point to be the other. There are only two possible answers to this question, depending on where you decide to place the H and V points. At this point, we do not know the angle that an observer would have to be at to make the shear stresses go away — we only know that such an orientation exists.

EXAMPLE 3. Consider an isotropic symmetric 2×2 matrix (i.e., a matrix that is simply a multiple of the 2×2 identity matrix). The following represents a state of hydrostatic tension of magnitude 3:

$$\begin{bmatrix} 3 & 0 \\ 0 & 3 \end{bmatrix}. \quad (2.15)$$

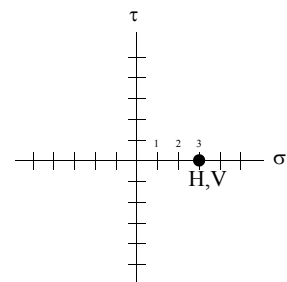


The H and V points for this matrix turn out to be identical:

$$\begin{aligned} \text{H: } & (3, 0) \\ \text{V: } & (3, 0). \end{aligned} \quad (2.16)$$

The H and V points will always be identical for any isotropic matrix. Conversely, if the H and V points coincide, then the matrix must be isotropic.

In this special case, the Mohr's circle degenerates to a single point. This means that, no matter how you look at this stress state, the matrix will always be given by Eq. (2.15). This is a highly exceptional situation given that matrix components normally change upon a change in reference frame.



By the way, noting that the shearing stress is zero on *any* plane, we conclude that any vector is an eigenvector of the matrix in Eq. (2.15), and the associated eigenvalue equals 3.

Coordinate transformations using Mohr's circle

Recall that the Mohr's circle represents a parametric plot of normal and shear stresses as they vary for different plane orientations. The following important property is proved in the Appendix:

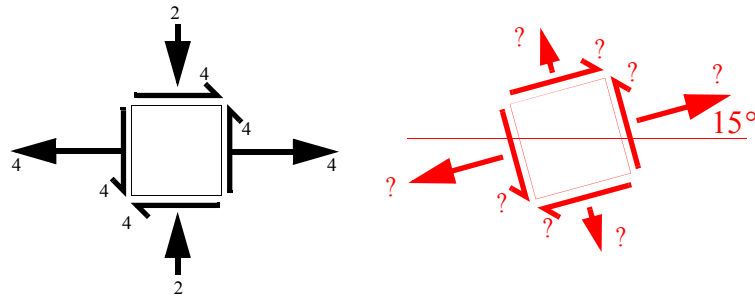
Whenever a plane is oriented at an angle θ measured counterclockwise from the laboratory horizontal, then the corresponding point on Mohr's circle will be at an angle 2θ measured in the same direction from the H-point on Mohr's circle.

The circled statement on page 9 is a special application of this statement. This property is the motivation for using a left-hand rule for signing the shear stresses; if a *right-hand* rule had been used, then an angle measured one way in the physical plane would be measured in the *opposite* way on Mohr's circle.

You can use the above property of Mohr's circle to perform coordinate transformations, as we will now illustrate via several examples.

EXAMPLE 4. Consider the following stress matrix referenced to the laboratory basis:

$$\begin{bmatrix} 4 & 4 \\ 4 & -2 \end{bmatrix}. \quad (2.17)$$

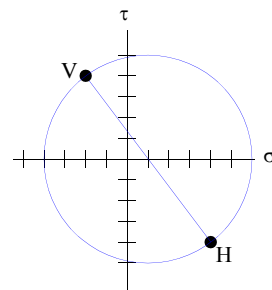


We wish to use Mohr's circle to determine the stress matrix for this stress state as seen by an observer who is rotated 15° counterclockwise from the laboratory orientation. In other words, we want to determine values for the question marks in the above figure.

SOLUTION: The matrix of Eq. (2.17) corresponds to the following H and V points:

$$\begin{aligned} \text{H: } & (4, -4) \\ \text{V: } & (-2, 4), \end{aligned} \quad (2.18)$$

from which Mohr's circle is constructed as shown. To find the stress state corresponding to $\theta = 15^\circ$ measured counterclockwise from the horizontal, we must measure $2\theta = 30^\circ$ counterclockwise from the H-point on Mohr's circle. If you have a protractor, this is a relatively easy task to do graphically, which explains why Mohr's circle was such a popular tool in the days before calculators.



Let's do this one analytically. From the known coordinates of the points H and V, we observe that the center of the Mohr's circle is located at

$$C_M = 1. \quad (2.19)$$

The radius of the Mohr's circle is

$$R_M = \sqrt{3^2 + 4^2} = 5. \quad (2.20)$$

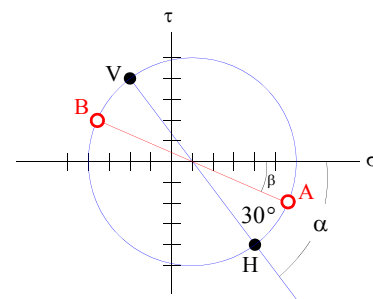
We also need the two angles marked α and β . Based on the coordinates of H, we see that

$$\alpha = \tan^{-1}\left(\frac{4}{3}\right) \approx 53.13^\circ. \quad (2.21)$$

Referring to the figure, β differs from α by 30° , so that

$$\beta = \alpha - 30^\circ = 23.13^\circ. \quad (2.22)$$

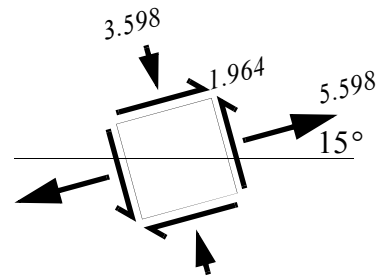
A simple geometrical inspection of the preceding figure shows that the coordinates of the points A and B are



$$\begin{aligned} \text{A: } & (C_M + R_M \cos \beta, -R_M \sin \beta) = (5.598, -1.964) \\ \text{B: } & (C_M - R_M \cos \beta, R_M \sin \beta) = (-3.598, 1.964). \end{aligned} \tag{2.23}$$

Consequently, the stress matrix and stress element as seen by an observer who is rotated 15° counterclockwise from the horizontal are now known. First we draw the stress element and, from there, we construct the matrix:

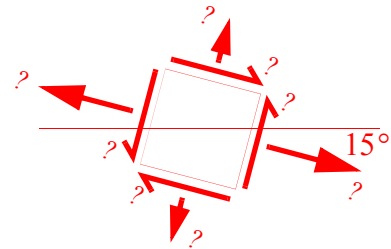
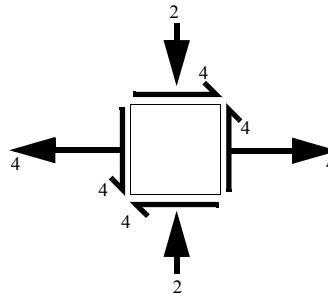
$$\begin{bmatrix} 5.598 & 1.964 \\ 1.964 & -3.598 \end{bmatrix}. \tag{2.24}$$



Even though this result was derived analytically, the Mohr's circle nevertheless provides an excellent means of visually verifying that analytical results are indeed reasonable. You can *look* at the drawing to see that the computed coordinates for A and B appear to be accurate.

Exercise 4. Again consider the stress state of Eq. (2.17):

$$\begin{bmatrix} 4 & 4 \\ 4 & -2 \end{bmatrix}. \tag{2.25}$$

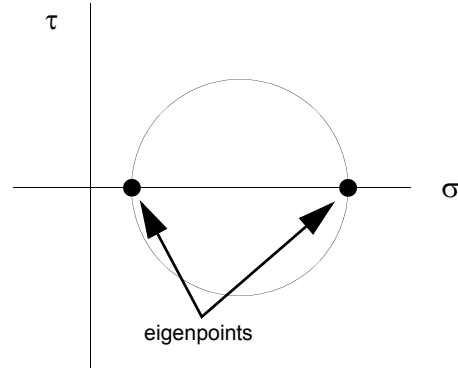


This time, use Mohr's circle to determine the stress matrix as seen by an observer who is rotated 15° *clockwise* from the laboratory orientation. In other words, determine values for the question marks in the above figure.

Eigensystem of a 2x2 matrix

The eigenvalues of a matrix are just the σ values at the two “**eigenpoints**” where Mohr's circle crosses the σ axis. If an analytical solution is desired for the eigenvalues and eigenvectors of a 2×2 matrix, there is a very easy formula. Specifically, suppose that the matrix is

$$\begin{bmatrix} a & b \\ b & c \end{bmatrix}. \quad (2.26)$$



The eigensystem of the above 2×2 matrix can be quickly determined by the following sequence of calculations:

Define: $d \equiv \frac{a-c}{2}$.

Center of Mohr's circle: $C_M \equiv \frac{a+c}{2}$.

Radius of Mohr's circle: $R_M \equiv \sqrt{d^2 + b^2}$.

Eigenvalues: $\lambda = C_M \pm R_M$.

Corresponding eigenvectors: $\begin{bmatrix} b + d \pm R_M \\ b - d \pm R_M \end{bmatrix}^\wedge$, where the “ \wedge ” indicates that the eigenvector must be normalized if so desired.

One disadvantage of the above procedural method is its lack of physical insight. You can use Mohr's circle to graphically check your calculations. Finding eigenvectors via Mohr's circle is done as a simple coordinate transformation in which the angle to the eigenvector is half of the angle from the H-point to the eigenpoint. This method is illustrated in the next example.

EXAMPLE 5. Consider the stress state of Eq. (2.17). Namely

$$\begin{bmatrix} 4 & 4 \\ 4 & -2 \end{bmatrix} \tag{2.27}$$

- (a) Find the orientations of the two planes on which the shear stress is maximized and determine the normal stress on those planes.
- (b) Use Mohr's circle to find the eigenvalues and eigenvectors of the matrix.

SOLUTION:

(a) The points of maximum shear stress are marked C and D in the figure at right. Recall from the preceding example that

$$\alpha = 53.13^\circ, \tag{2.28}$$

Inspecting the geometry of the circle, point C is at an angle $\alpha + 90^\circ$ measured *counterclockwise* from H. Recall that an angle measured from the H-point on Mohr's circle corresponds to *half* as large of an angle in the physical plane. Hence, the physical plane corresponding to point "C" must be at an angle

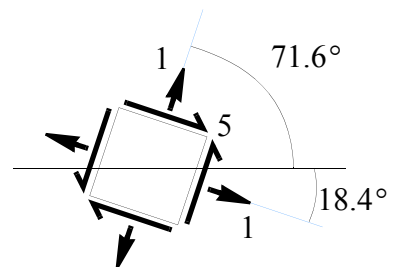
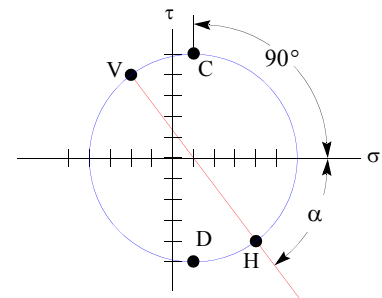
$$\frac{\alpha + 90^\circ}{2} \approx 71.6^\circ, \tag{2.29}$$

measured *counterclockwise* from the horizontal. Notice that we measured in the same direction (counterclockwise) from "H" in both the physical plane and on Mohr's circle. The coordinates of point C are (1,5). Hence, the shear stress on this plane is of magnitude 5 and the normal stress at that orientation equals 1. The shear at point C is *positive* 5, so the shear on the "C-face" (oriented at 71.6°) must be drawn positive by the *left-* hand rule.

Similarly, the point D on Mohr's circle is located at an angle $90^\circ - \alpha$, measured *clockwise* from H. Consequently, the physical plane corresponding to point D must be at *half* that angle:

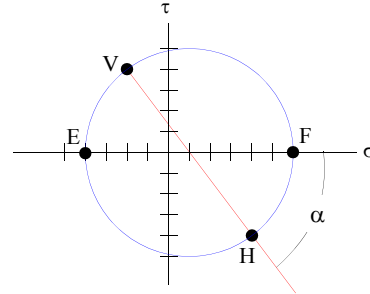
$$\frac{90^\circ - \alpha}{2} \approx 18.4^\circ, \tag{2.30}$$

This angle is to be measured *clockwise* from the horizontal because that's how we measured from the H-point on Mohr's circle. Notice that you may choose to measure clockwise or counterclockwise as you see fit — you only need to be consistent.



The points C and D are diametrically opposite each other on Mohr's circle, so (recalling the circled statement on page 9) it should come as no surprise that the two planes of maximum shear differ from each other by exactly 90° in the physical plane. The stress element at right shows both of these planes of maximum shear.

(b) For this part of the question, we seek the eigenvectors of the matrix. When viewed as a stress matrix, this means we seek the orientation of planes on which the shear stress is zero. The points marked E and F on the Mohr's circle at right correspond to zero shear stress. The normal stresses at these points must therefore be the eigenvalues of the matrix; namely,



$$\begin{aligned} \text{Eigenvalue for point E:} \quad \lambda_E &= -4 \\ \text{Eigenvalue for point F:} \quad \lambda_F &= 6. \end{aligned} \quad (2.31)$$

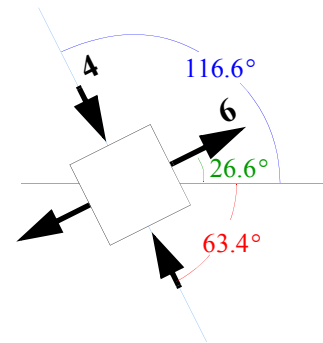
Point F is located at an angle $\alpha \approx 53.13^\circ$ measured counterclockwise from the H point on Mohr's circle. Therefore, the plane corresponding to point F has an outward unit normal that makes an angle half as large: $\alpha/2 = 26.6^\circ$. This angle is measured from the physical horizontal in the same direction that it was measured from the H-point on Mohr's circle, namely counterclockwise. The physical plane associated with the point F has an outward unit normal that makes an angle of 26.6° with the horizontal. This unit normal is the eigenvector associated with the eigenvalue λ_F . Thus, the eigenvector corresponding to point F is

$$\begin{Bmatrix} \cos(26.6^\circ) \\ \sin(26.6^\circ) \end{Bmatrix} = \begin{Bmatrix} 0.894 \\ 0.447 \end{Bmatrix}. \quad (2.32)$$

The point E is diametrically opposite F on Mohr's circle, so the eigenvector for E must be perpendicular to that for F. Hence, the eigenvector associated with point E must be

$$\begin{Bmatrix} -\sin(26.6^\circ) \\ \cos(26.6^\circ) \end{Bmatrix} = \begin{Bmatrix} -0.447 \\ 0.894 \end{Bmatrix}. \quad (2.33)$$

The stress element at right is oriented in the principal directions. Of course, we could have alternatively computed the second eigenvector in exactly the same way as we did the first eigenvector. To do this, it is probably easiest to measure the angle counterclockwise. Specifically, the second eigenvalue (at point E) is at an angle $\alpha + 180^\circ$ measured counterclockwise from the H-point on Mohr's circle. Hence, in the physical plane, the second eigenvector makes an angle $(\alpha + 180^\circ)/2 = 116.6^\circ$ measured counterclockwise from the physical horizontal. Thus, the second eigenvector (corresponding to point E) is



$$\begin{Bmatrix} \cos(116.6^\circ) \\ \sin(116.6^\circ) \end{Bmatrix} = \begin{Bmatrix} -0.447 \\ 0.894 \end{Bmatrix}, \quad (2.34)$$

which is identical to Eq. (2.33), as it should be.

It is perfectly legitimate to measure angles in a clockwise direction rather than counterclockwise. For example, the point E is at an angle of $180^\circ - \alpha$ measured *clockwise* from point H. Thus, the *physical* plane associated with E must be oriented at an angle of $(180^\circ - \alpha)/2 = 63.4^\circ$ which must also be measured *clockwise* from the horizontal, as shown in the above figure. The result for the eigenvector is the same.

Finally, note that one could alternatively measure angles from the V-point on Mohr's circle. The corresponding physical plane would have an orientation at half as large of an angle, *measured from the vertical* in the same direction.

As a final check, let's apply the procedural method given on page 16 to see if we obtain the same eigensystem.

Comparing Eq. (2.26) with (2.27) we set $\begin{bmatrix} a & b \\ b & c \end{bmatrix} = \begin{bmatrix} 4 & 4 \\ 4 & -2 \end{bmatrix}$ and therefore identify

$$a = 4, \quad b = 4, \quad \text{and} \quad c = -2.$$

$$\text{Define: } d \equiv \frac{a-c}{2} = \frac{4-(-2)}{2} = 3.$$

$$\text{Center of Mohr's circle: } C_M \equiv \frac{a+c}{2} = \frac{4+(-2)}{2} = 1.$$

$$\text{Radius of Mohr's circle: } R_M \equiv \sqrt{d^2 + b^2} = \sqrt{3^2 + 4^2} = 5.$$

$$\text{Eigenvalues: } \lambda = C_M \pm R_M = 1 \pm 5, \text{ giving } \lambda_1 = 6 \text{ and } \lambda_2 = -4.$$

$$\text{Corresponding eigenvectors: } \begin{bmatrix} b + d \pm R_M \\ b - d \pm R_M \end{bmatrix}^\wedge = \begin{bmatrix} 4 + 3 \pm 5 \\ 4 - 3 \pm 5 \end{bmatrix}^\wedge = \begin{bmatrix} 7 \pm 5 \\ 1 \pm 5 \end{bmatrix}^\wedge.$$

$$\text{So the first eigenvector is } \begin{bmatrix} 7 + 5 \\ 1 + 5 \end{bmatrix}^\wedge = \begin{bmatrix} 12 \\ 6 \end{bmatrix}^\wedge = \frac{1}{\sqrt{5}} \begin{bmatrix} 2 \\ 1 \end{bmatrix} = \begin{bmatrix} 0.8944 \\ 0.4472 \end{bmatrix}, \text{ which agrees}$$

with the result in Eq. (2.32). Likewise, the second eigenvector is

$$\begin{bmatrix} 7 - 5 \\ 1 - 5 \end{bmatrix}^\wedge = \begin{bmatrix} 2 \\ -4 \end{bmatrix}^\wedge = \frac{1}{\sqrt{5}} \begin{bmatrix} 1 \\ -2 \end{bmatrix} = \begin{bmatrix} 0.4472 \\ -0.8944 \end{bmatrix} \text{ in agreement with Eq. (2.34) with the}$$

exception of the multiple of -1 , which is inconsequential since eigenvectors can be multiplied by -1 without loss in generality.

The fabulous Pole Point

In this age of readily-available scientific computers, the usefulness of Mohr's circle mostly lies in its ability to give you quick graphical estimates. You might, for example, be sitting in a technical seminar and need to quickly determine whether a matrix has any negative eigenvalues, or you may need an estimate of the maximum shear stress. For such purposes, Mohr's circle can't be beat.

One drawback with the classical version of Mohr's circle is that angles in physical space map to *twice* the angle on Mohr's circle. Furthermore, the angle on Mohr's circle is measured from the H-point, which itself might be at an awkward or difficult-to-visualize location. The pole point* is a little-known extension to Mohr's circle that rectifies these problems.

To construct the pole point, all you do is draw a horizontal line through the H-point and a vertical line through the V-point. These two lines will always intersect the Mohr's circle at the same location. This special point is called the "pole point" and is labeled "P."

The remarkable property of the pole point is that you can draw a line from the pole point to some other point on Mohr's circle and the orientation of that line will exactly coincide with the *actual* orientation of the associated plane in physical space — it won't differ by a factor of 2, and (just like the angle in physical space) it will be measured relative to the horizontal in the Mohr diagram rather than relative to the H-point. You can then draw stress elements with the proper orientation directly on Mohr's circle. These concepts are best explained via examples.

* See, for example,

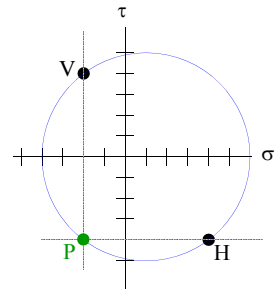
Allison, I. (1984) The pole of the Mohr diagram. *J. Struct. Geol.* **6**, 331-333.

Lisle, R.J. (1992) Strain analysis by simplified Mohr Circle construction. *Annals Tectonicae* **5**, 102-117.

EXAMPLE 6. Rework example 4 using the pole point.

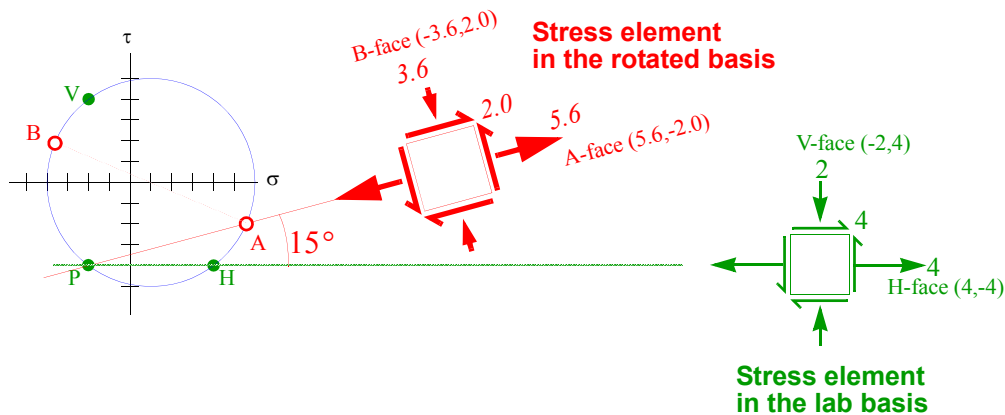
SOLUTION: Recall the matrix and Mohr's circle from Example 4:

$$\begin{bmatrix} 4 & 4 \\ 4 & -2 \end{bmatrix}. \tag{2.35}$$



The pole point P is constructed by drawing a horizontal line through H and a vertical line through V, as shown in the figure.

Recall that example 4 asked for the expression of the stress matrix as seen by an observer who is rotated 15° from the horizontal.



To solve this problem graphically, you use a protractor to draw a line *that passes through the pole point P* at an angle of 15° from the horizontal. As long as your drawing is moderately accurate, you can estimate the coordinates of the point “A” where this line passes through Mohr's circle. This point “A” is exactly the same as the point A in Example 4! Point A corresponds to the normal/shear stress pair on the plane whose normal is at 15° from the physical horizontal! We simply “eyeball” the drawing to estimate the coordinates of point A as roughly

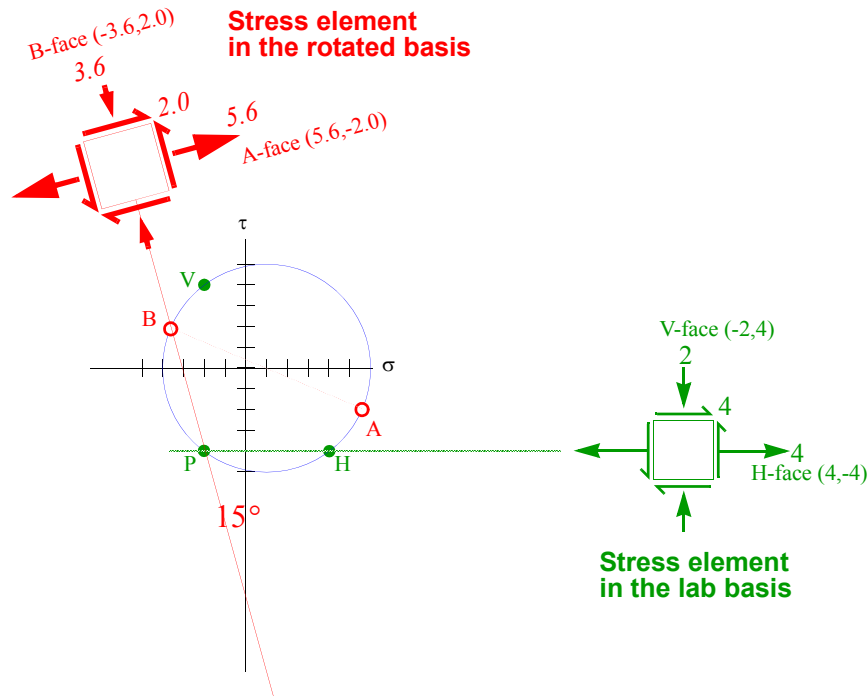
$$A: (5.6, -2.0). \tag{2.36}$$

Recalling Eq. (2.23), the exact solution for the normal and shear stresses on this face were (5.598, -1.964), we conclude that the pole point is indeed a very powerful estimation tool. Of course point “A” corresponds only to the face of the stress element whose normal is at 15°. To draw the full stress element, we again recall that the stresses on other face are determined by reading the coordinates of point “B” *diametrically opposite* from point A:

$$B: (-3.6, 2.0). \tag{2.37}$$

The normal stress on this face is negative, so it is shown as compressive in the stress element. The shear stress at point B is positive, so it is drawn to be positive by the *left-hand rule*.

By the way, we would have ended up with the same stress element if we had instead drawn a line from the pole point to point B in the figure. The resulting sketch would then look like this:

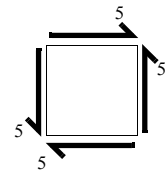


Exercise 5. Rework exercise 4 using the pole point. Use graphical methods only — make an *accurate* drawing on grid paper and read off the relevant coordinates from your figure. Don't use trigonometry.

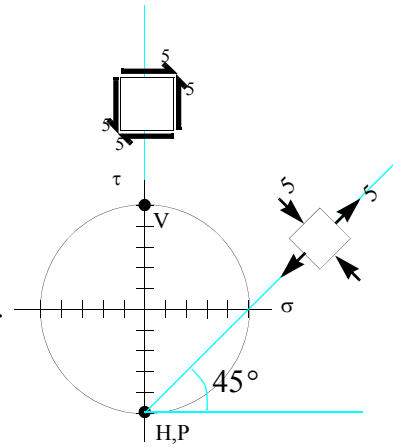
EXAMPLE 7. Consider the matrix of Eq. (2.12):

$$\begin{bmatrix} 0 & 5 \\ 5 & 0 \end{bmatrix}.$$

(2.38)



This matrix is interesting because, if you draw a horizontal line through the H-point and a vertical line through the V-point, it turns out that the pole point P is in the same spot as the H-point. There is nothing wrong with this situation. All the previous comments about the pole point remain valid. For example, you could immediately observe that the principal directions for this matrix are oriented at $\pm 45^\circ$ relative to the physical laboratory basis. You can draw *both* the original stress element of Eq. (2.38) *and* the principal stress element (on which shear stresses are zero) directly on the Mohr's circle as shown. The max eigenvalue equals 5, and we elected to draw the line from P through this point on Mohr's circle. Hence, the normal stress on this line equals +5. The normal stress on the other face of the stress element is -5 , which comes from looking at the diametrically opposite point on Mohr's circle.



Exercise 6. Using only a straight-edge and a protractor, graphically solve the problem of Example 5 by using the pole point. Show the pole point and the two stress elements (max shear and zero shear) directly on your drawing (as was done in the examples 6 and 7).

Application of the pole point to strain rosettes

Strain is a symmetric 3×3 tensor that quantifies deformation, but it unfortunately is defined in many different ways by many different people. The deformation gradient tensor $\underline{\underline{F}}$ (discussed in great detail later) is a superior measure of deformation because its definition is universally accepted and, like strain, it incorporates material size and shape changes, but it also characterizes overall material rotation (something a strain measure cannot do). The deformation gradient tensor is defined so that an infinitesimal material element $d\underline{\underline{X}}$ will deform to a new orientation and length such that

$$d\underline{\underline{x}} = \underline{\underline{F}} \bullet d\underline{\underline{X}} \quad (2.39)$$

The square of the initial length is $L_o^2 = d\underline{\underline{X}} \bullet d\underline{\underline{X}}$ and the square of the deformed length is $L^2 = d\underline{\underline{x}} \bullet d\underline{\underline{x}}$. Consequently,

$$d\underline{\underline{x}} \bullet d\underline{\underline{x}} = d\underline{\underline{X}} \bullet \underline{\underline{U}}^2 \bullet d\underline{\underline{X}}, \text{ where } \underline{\underline{U}} = +[\underline{\underline{F}}^T \bullet \underline{\underline{F}}]^{1/2} \quad (2.40)$$

Stated differently,

$$\begin{aligned} \lambda_M^2 &= \underline{\underline{M}} \bullet \underline{\underline{U}}^2 \bullet \underline{\underline{M}}, \\ \text{where } \lambda_M &= \frac{L}{L_o} \text{ and } \underline{\underline{M}} \text{ is a unit vector in the direction of } d\underline{\underline{X}} \end{aligned} \quad (2.41)$$

The “reference stretch” tensor $\underline{\underline{U}}$, characterizes the size and shape change associated with the deformation; it loses information about material rotation. All of the commonly used strain definitions can be expressed in terms of $\underline{\underline{U}}$ by an expression of the form

$$\underline{\underline{\epsilon}} = \frac{1}{k} [\underline{\underline{U}}^k - \underline{\underline{I}}] \quad (2.42)$$

Here, k is called the Seth-Hill parameter. Choosing $k = 1$ will give the engineering strain analogous to the linear strain defined with respect to initial and final lengths of a uniaxial specimen by $\epsilon = (L - L_o)/L_o$. Choosing $k = -1$ will give a strain analogous to $\epsilon = (L - L_o)/L$. Choosing $k \rightarrow 0$ in the limit will give the logarithmic strain analogous to $\epsilon = \ln(L/L_o)$. Evaluating $\underline{\underline{U}}$ in Eq. (2.40) involves taking the square root of a tensor, which is an onerous task requiring an eigenvalue decomposition. However, if only the strain is desired, the eigenvalue decomposition can be avoided if an *even* nonzero Seth-Hill parameter is used. The choice $k = 2$ corresponds to the Lagrange strain that is commonly used in numerical analysis; with this choice, $\underline{\underline{U}}^k = \underline{\underline{U}}^2 = \underline{\underline{F}}^T \bullet \underline{\underline{F}}$. The Lagrange strain is easy to compute, but one should be cautioned that it is unstable under large compressions if a linear elasticity model is used. The choice $k = -2$ also avoids the eigenvalue decomposition, and it is stable in compression but unstable in tension.* All strain definitions are approximately equivalent when material stretching is small.

* The only choice that is stable in both compression and tension is the logarithmic strain ($k = 0$). Any choice for k can be made stable if a nonlinear elasticity model is used.

Clearly, the choice of strain measure is a murky one indeed. All of the strain definitions are functions of the (well-defined) stretch, we will outline below how to compute the stretch tensor. Once you have that, you can compute whatever strain definition you seek.

Recall our formula for the fiber stretch:

$$\lambda_M^2 = \underline{M} \cdot \underline{U}^2 \cdot \underline{M},$$

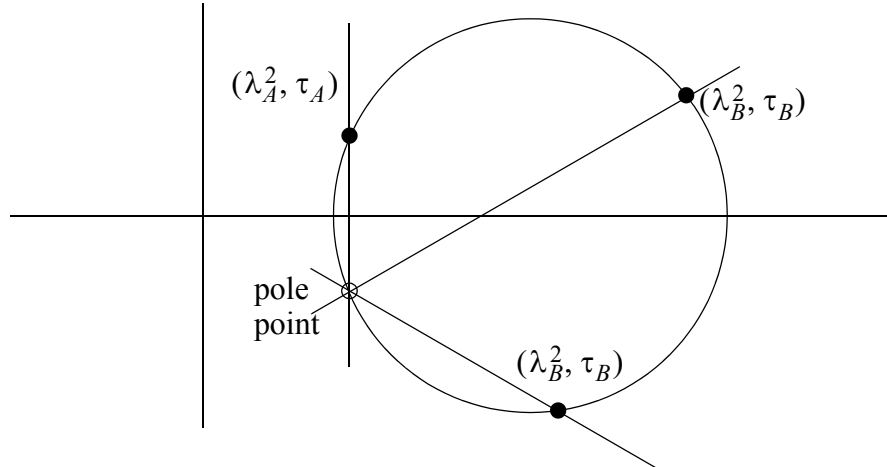
$$\text{where } \lambda_M = \frac{L}{L_o} \text{ and } \underline{M} \text{ is a unit vector in the direction of } d\underline{X} \quad (2.43)$$

This formula is the basis for linear strain gages, which are basically wires that increases electrical resistance when stretched.* If a gage is glued to a surface so that the gage is parallel to some direction \underline{M} , then it will move with the surface upon deformation, causing it to change length and change electrical resistance. Most gage manufactures will convert this resistance change to a linear engineering strain, ϵ^g , so the gage stretch can be readily computed by $\lambda^g = \epsilon^g + 1$. Most gages will respond nonlinearly under large deformation, so an independent calibration experiment might be required to convert the strain reported by the gage to the actual stretch experienced by the material. For our purposes, we will presume that you have available to you a set of gages from which you can determine accurate stretches.

Note that the gage will output only voltages associated with length change. The gage does not directly measure reorientation of the material. However, when measuring strain in a plane, the reorientation may be inferred by using a third strain gage. Typically the gages are glued one on top of another at a point, differing in orientation by 60° . Let the first strain gage (gage "A") point in the vertical-direction. Let the second (gage "B") point 30° above the horizontal and let the third (gage "C") point 30° below horizontal. Equation (2.43) tells us that λ_M^2 equals the normal component of \underline{U}^2 . There is no information

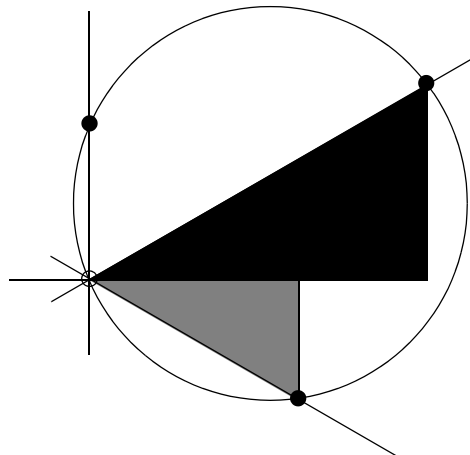
* To amplify the effect, the wire is typically arranged in a zig-zag pattern, with most of the wire being parallel.

about the shear components. We wish to construct the Mohr circle for \underline{U}^2 given only the three gage stretches and no direct information about shear strains (the information is there, but not measured explicitly). If we *did* know the shear components of \underline{U}^2 , then the Mohr's circle might look like this:

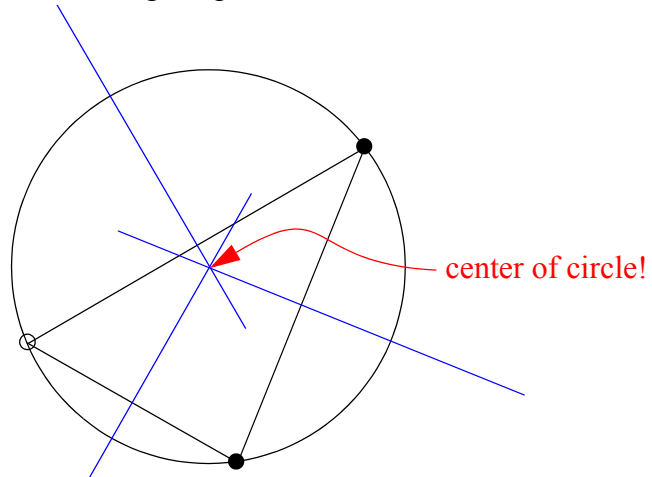


By the nature of the pole point, we know that a straight line emanates from the pole point to each point on the Mohr's circle with a slope given by the gage orientation (vertical, 30° above horizontal, and 30° below horizontal).

Unfortunately, the gages do *not* give us any values for shear components. From the geometry of the Mohr's circle, though, we *can* determine the values of τ_k relative to the pole point. A temporary origin is set up to coincide with the pole point so that the above drawing becomes:



In this drawing, the horizontal width of the black triangle equals $\lambda_2^2 - \lambda_1^2$, and the vertical height of this triangle is determined by intersecting with the line angled at $+30^\circ$. The horizontal width of the gray triangle is $\lambda_2^2 - \lambda_1^2$, and its vertical height may be found by intersecting with the line angled at -30° . These two intersection points, together with the pole point itself, constitute a set of three points that must lie on the Mohr's circle. Any circle is fully determined by three points. Graphically, the center of the circle can be found the intersection of bisectors of chords connecting the points like this:



Once the center of Mohr's circle has been found in this manner, the temporary origin can be discarded and the genuine origin of Mohr's circle may be placed such that the horizontal passes through the circle's center. The vertical axis in Mohr's diagram is determined from the reading of gage "A." From there, the coordinates of the principal values can be read off of the graph in the ordinary manner.

EXAMPLE 8. Suppose that the three gages of a strain rosette output engineering strains of $\varepsilon_A = 0.1$, $\varepsilon_B = 0.2$, $\varepsilon_C = 0.5$. Find the engineering and logarithmic strain tensors with respect to a basis for which the 2-direction is aligned with gage "A."

SOLUTION: The gages output engineering strains. The associated stretches are

$$\lambda_A = \varepsilon_A + 1 = 1.1, \text{ therefore, } \lambda_A^2 = 1.21 \quad (2.44)$$

$$\lambda_B = \varepsilon_B + 1 = 1.2, \text{ therefore, } \lambda_B^2 = 1.44 \quad (2.45)$$

$$\lambda_C = \varepsilon_C + 1 = 1.5, \text{ therefore, } \lambda_C^2 = 2.25 \quad (2.46)$$

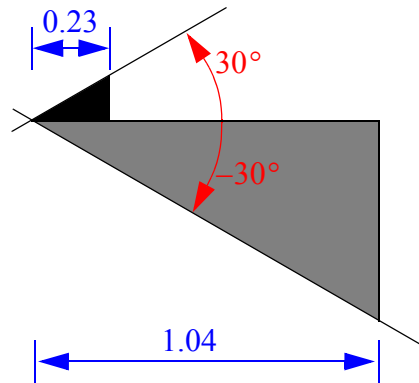
Consequently, the width of the "black" triangle will be

$$\lambda_B^2 - \lambda_A^2 = 0.23 \quad (2.47)$$

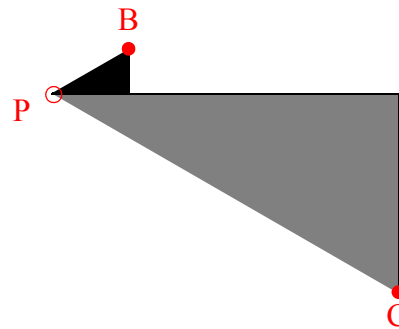
The width of the "gray" triangle is

$$\lambda_C^2 - \lambda_A^2 = 1.04 \tag{2.48}$$

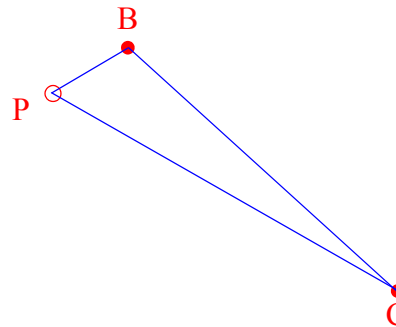
Drawing these two triangles with a common acute vertex gives the picture shown at right.



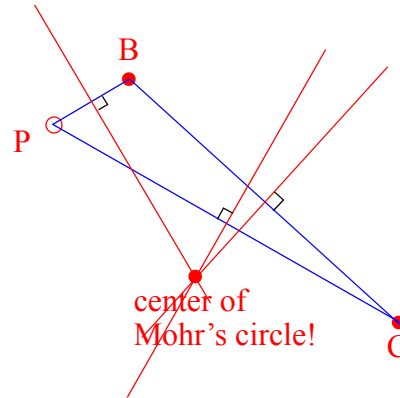
Three points on the Mohr's circle (the pole point P and the points associated with gages B and C) are identified by the acute vertices of the triangles as shown.



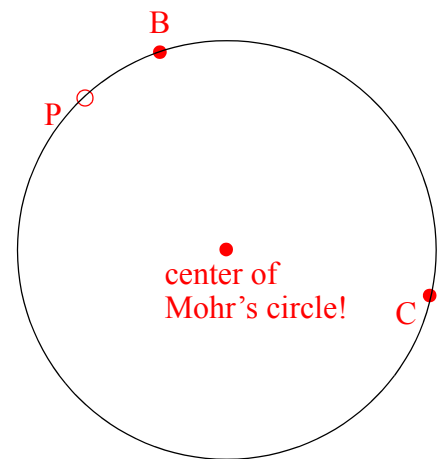
The black and gray triangles can now be discarded leaving only the points behind. Chords connecting the points can be drawn as shown:



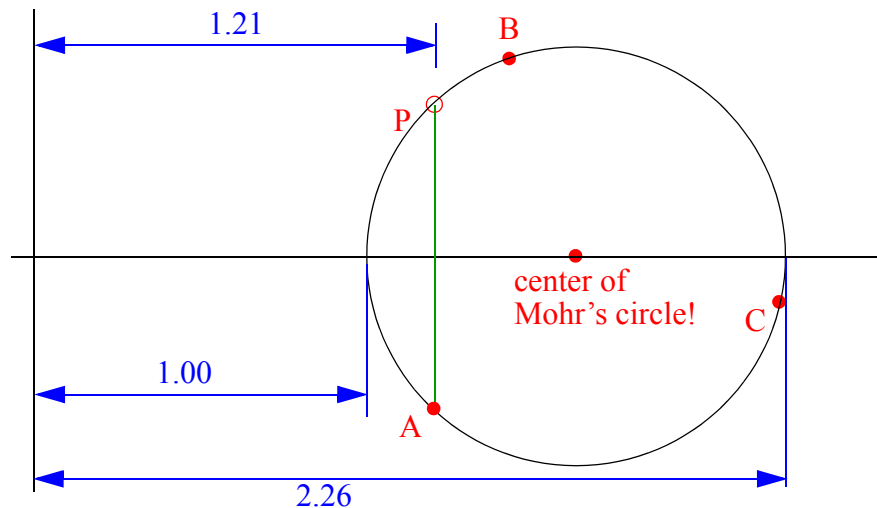
Bisectors of the chords are constructed. The three bisectors will always intersect at the same location.



The chords and bisectors can now be discarded, leaving behind only the three points P, B, and C and the center of Mohr's circle. Draw the circle to pass through the three points.



Now that the center is known, the horizontal axis of Mohr's diagram can be drawn to pass through the center of the circle as shown below. The vertical axis can now also be positioned so that the pole point P is a distance $\lambda_A^2 = 1.21$ away. The point on Mohr's circle corresponding to gage A is found by dropping a vertical from P.



This completes the graphical construction of the Mohr's circle for \underline{U}^2 . Since \underline{U}^2 is a positive definite tensor, the entire Mohr's circle will *always* be contained entirely to the right of the vertical axis.

The eigenvalues of \underline{U}^2 are at the extreme ends where the circle intersects the horizontal axis. Reading off these values graphically (using a ruler) gives

$$\lambda_{\min}^2 = 1.00 \text{ or } \lambda_{\min} = 1.00 \text{ and therefore } \ln \lambda_{\min} = 0.0 \tag{2.49}$$

$$\lambda_{\max}^2 = 2.26 \text{ or } \lambda_{\max} = 1.50 \text{ and therefore } \ln \lambda_{\max} = 0.41 \tag{2.50}$$

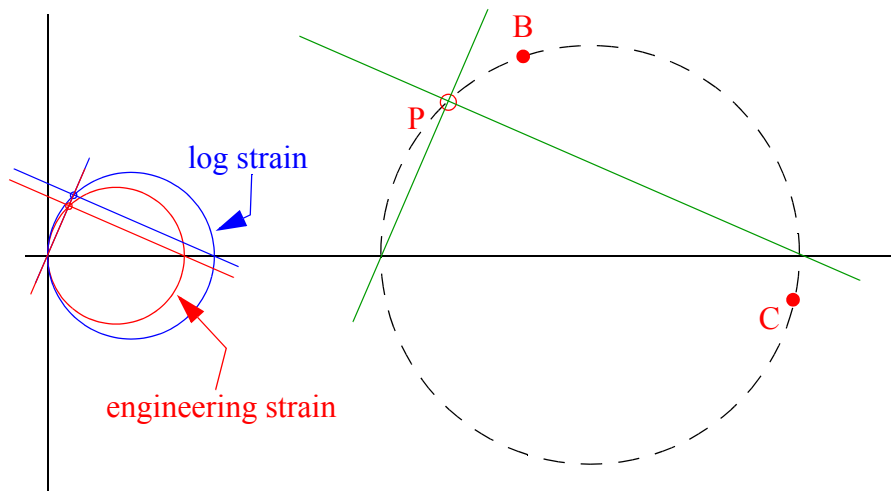
Therefore, with respect to the principal basis, the logarithmic strain tensor is given by

$$\begin{bmatrix} 0.0 & 0 \\ 0 & 0.41 \end{bmatrix} \tag{2.51}$$

With respect to the principal basis, the *engineering* strain tensor is

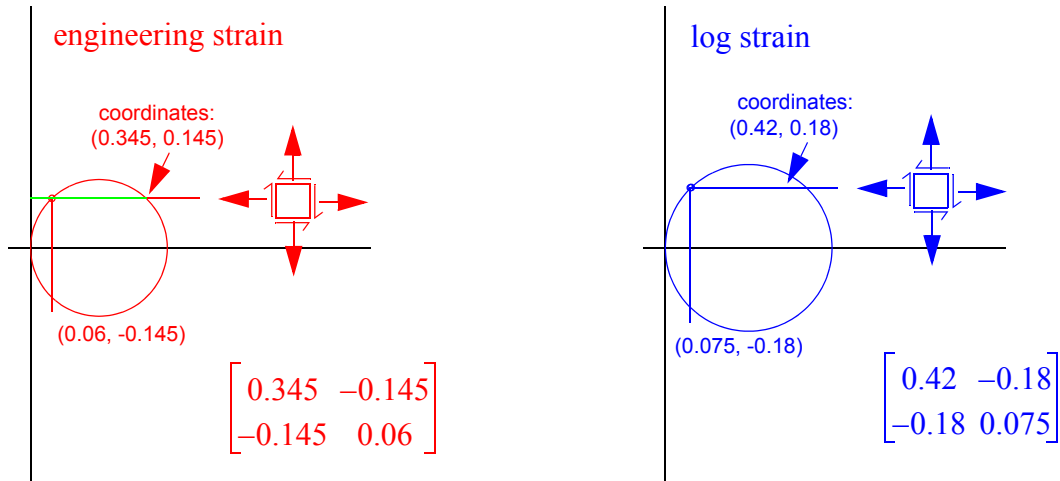
$$\begin{bmatrix} 0.0 & 0 \\ 0 & 0.50 \end{bmatrix} \tag{2.52}$$

The Mohr's circles for these strain tensors are shown below:



This example, unfortunately, did not ask for the strains in the principal basis. It asked for the strains relative to a basis for which the 2-direction is aligned with gage "A."

The orientations of the principal directions of \underline{U}^2 are shown above in green. The principal directions of strain are the same as those of \underline{U}^2 . Consequently, the pole points for the strain circles can be found by passing parallel lines through the eigenvalues as shown. With the pole points known, the strain tensors relative to the vertical gage "A" can be found by passing vertical and horizontal lines through the pole points and then reading off the values. The process is shown below for each strain individually:



Double checking the result. With rosette stretches of 1.1, 1.2, and 1.5, we can draw three line segments of these lengths as shown:

These lines can be assembled into a triangle with the line for gage A remaining vertical

The vector for gage B is

$$\mathbf{g}_B = \{1.18, 0.193\}$$

The vector for gage C is

$$\mathbf{g}_C = \{1.18, -0.889\}$$

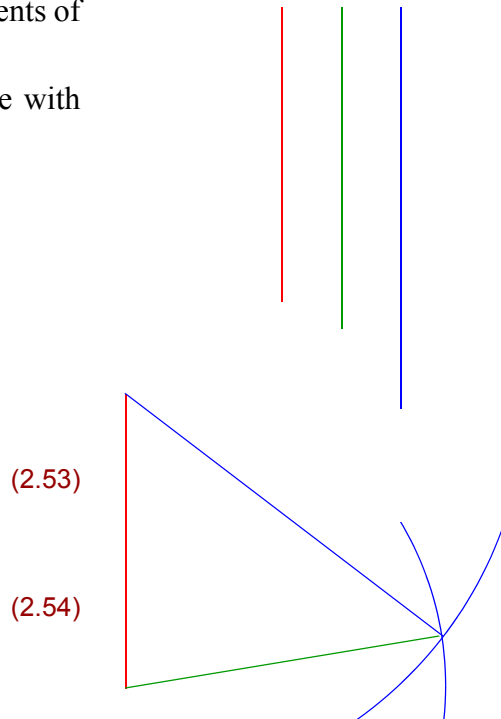
These vectors were initially given by

$$G_B = \left\{ \frac{\sqrt{3}}{2}, \frac{1}{2} \right\} \tag{2.53}$$

$$G_C = \left\{ \frac{\sqrt{3}}{2}, -\frac{1}{2} \right\} \tag{2.54}$$

The duals for these vectors are

$$G^B = \left\{ \frac{1}{\sqrt{3}}, -1 \right\} \tag{2.55}$$



$$G^C = \left\{ \frac{1}{\sqrt{3}}, 1 \right\} \quad (2.56)$$

The deformation gradient is

| $F = g_B G^B + g_C G^C$ **Reb: finish this. Compute F , get U** (2.57)

Mohr's circle for three-dimensional states of "stress"

Consider a full 3×3 "stress" matrix:

$$\begin{bmatrix} \sigma_{11} & \sigma_{12} & \sigma_{13} \\ \sigma_{21} & \sigma_{22} & \sigma_{23} \\ \sigma_{31} & \sigma_{32} & \sigma_{33} \end{bmatrix}. \quad (2.58)$$

The matrix is symmetric if $\sigma_{ij} = \sigma_{ji}$. The traction vector on a plane with unit normal \mathbf{n} is given by the operation $\underline{\underline{\sigma}} \cdot \mathbf{n}$. The normal component of traction is

$$\sigma = \mathbf{n} \cdot \underline{\underline{\sigma}} \cdot \mathbf{n}. \quad (2.59)$$

The magnitude of the shear stress on the plane is

$$\tau = \sqrt{\|\underline{\underline{\sigma}} \cdot \mathbf{n}\|^2 - \sigma^2}. \quad (2.60)$$

For convenience, we can always set up a laboratory basis that is aligned with the principal directions of stress. In terms of the principal basis,

$$[\underline{\underline{\sigma}}] = \begin{bmatrix} \sigma_1 & 0 & 0 \\ 0 & \sigma_2 & 0 \\ 0 & 0 & \sigma_3 \end{bmatrix}. \quad (2.61)$$

Furthermore, we can select the ordering for the basis such that $\sigma_1 \geq \sigma_2 \geq \sigma_3$. Let $\{n_1, n_2, n_3\}$ be the components of the unit vector \mathbf{n} with respect to the principal basis. Then Eqs. (2.59) and (2.61) become

$$\sigma = \sigma_1 n_1^2 + \sigma_2 n_2^2 + \sigma_3 n_3^2 \quad (2.62)$$

and

$$\tau^2 = \sigma_1^2 n_1^2 + \sigma_2^2 n_2^2 + \sigma_3^2 n_3^2 - \sigma^2. \quad (2.63)$$

The vector \mathbf{n} has unit magnitude, so its components must satisfy

$$n_1^2 + n_2^2 + n_3^2 = 1. \quad (2.64)$$

The above three equations may be solved for n_1^2 , n_2^2 , and n_3^2 to give

$$\begin{aligned} n_1^2 &= \frac{\tau^2 + (\sigma - \sigma_2)(\sigma - \sigma_3)}{(\sigma_1 - \sigma_2)(\sigma_1 - \sigma_3)} \geq 0 \\ n_2^2 &= \frac{\tau^2 + (\sigma - \sigma_3)(\sigma - \sigma_1)}{(\sigma_2 - \sigma_3)(\sigma_2 - \sigma_1)} \geq 0 \\ n_3^2 &= \frac{\tau^2 + (\sigma - \sigma_1)(\sigma - \sigma_2)}{(\sigma_3 - \sigma_1)(\sigma_3 - \sigma_2)} \geq 0. \end{aligned} \quad (2.65)$$

Ordering the principal stresses* so that $\sigma_1 \geq \sigma_2 \geq \sigma_3$, we may write these equations in the form

$$\begin{aligned}\tau^2 + (\sigma - \sigma_2)(\sigma - \sigma_3) &\geq 0 \\ \tau^2 + (\sigma - \sigma_3)(\sigma - \sigma_1) &\leq 0 \\ \tau^2 + (\sigma - \sigma_1)(\sigma - \sigma_2) &\geq 0.\end{aligned}\tag{2.66}$$

These inequalities may be re-written

$$\begin{aligned}\tau^2 + [\sigma - C_{23}]^2 &\geq R_{23}^2, \text{ where } C_{23} \equiv \frac{1}{2}(\sigma_2 + \sigma_3) \text{ and } R_{23} \equiv \frac{1}{2}(\sigma_2 - \sigma_3) \\ \tau^2 + [\sigma - C_{31}]^2 &\leq R_{31}^2, \text{ where } C_{31} \equiv \frac{1}{2}(\sigma_3 + \sigma_1) \text{ and } R_{31} \equiv \frac{1}{2}(\sigma_3 - \sigma_1) \\ \tau^2 + [\sigma - C_{12}]^2 &\geq R_{12}^2, \text{ where } C_{12} \equiv \frac{1}{2}(\sigma_1 + \sigma_2) \text{ and } R_{12} \equiv \frac{1}{2}(\sigma_1 - \sigma_2).\end{aligned}\tag{2.67}$$

The first of these equations says that the (τ, σ) shear and normal stresses on any plane will fall outside the circle with radius R_{23} centered at C_{23} . The second inequality says that the same (τ, σ) point must also lie *inside* the circle of radius R_{31} centered at C_{31} . Recalling that we have ordered the principal stresses from largest to smallest, this circle is the largest circle that can be formed between any two of the eigenvalues. The final inequality says that the (τ, σ) point must lie *outside* the circle of radius R_{12} centered at C_{12} .

Thus, to satisfy all of the above inequalities simultaneously, the point (σ, τ) on the Mohr diagram must lie within a region bounded by the three circles between the principal stress values. This is an extremely useful result for determining the maximum shear on a plane of arbitrary orientation.

* Actually, the analysis as shown requires the principal values to be distinct to avoid division by zero, but the reader is asked to verify that the same results still go through when there are repeated eigenvalues.

EXAMPLE 9. Figure 2.3 shows the results of a numerical experiment in which about 7400 unit normals were generated at random. For each unit normal generated by the computer program, the corresponding (σ, τ) point of Eqs. (2.59) and (2.60) was computed using the matrix

$$[\sigma] = \begin{bmatrix} 1 & 0 & 0 \\ 0 & 2 & 0 \\ 0 & 0 & 4 \end{bmatrix}. \quad (2.68)$$

This procedure produces a set of 7400 (σ, τ) points that could then be plotted on the Mohr diagram. The resulting distribution of (σ, τ) points shown in Fig. 2.3 verifies our interpretation of Eq. (2.67).

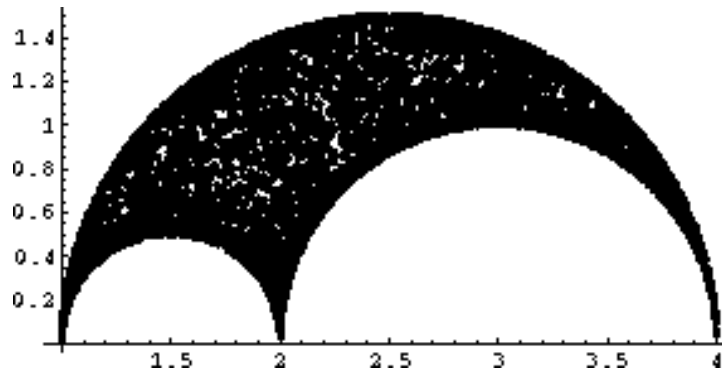


Figure 2.3. 3D Mohr diagram for 3x3 symmetric matrices. For this example, the principal values of the $[\sigma]$ matrix were $\sigma_1=4$, $\sigma_2=2$, and $\sigma_3=1$.

Application to planar “stress” states

The three-dimensional Mohr’s circle is a very useful for determining maximum shear for planar stress problems the 1-2 plane where the “out-of-plane” shears are known to be zero and the stress state is therefore of the form

$$[\sigma] = \begin{bmatrix} \sigma_{11} & \sigma_{12} & 0 \\ \sigma_{21} & \sigma_{22} & 0 \\ 0 & 0 & \sigma_{33} \end{bmatrix}. \quad (2.69)$$

One of the principal values of this matrix is clearly σ_{33} . The Mohr’s circle for the upper 2×2 submatrix is plotted as usual. Then two *additional* Mohr’s circles are drawn so that they pass through σ_{33} and the two principal values of the 2×2 submatrix.

Let λ_1 and λ_2 denote the principal values of the 2×2 submatrix, and order them such that $\lambda_1 > \lambda_2$. As illustrated in Fig. 2.4, there are three possible orderings for the third eigenvalue:

$$\lambda_1 \geq \lambda_2 \geq \sigma_{33}, \quad \lambda_1 \geq \sigma_{33} \geq \lambda_2, \quad \text{and} \quad \sigma_{33} \geq \lambda_1 \geq \lambda_2. \quad (2.70)$$

Referring to Fig. 2.4, the largest shear stress in the material must equal the radius of the largest Mohr's circle. This maximum shear stress is determined by the largest difference between principal values. Thus, even for planar stress states, the out-of-plane stress must be considered when determining maximum shear stress.

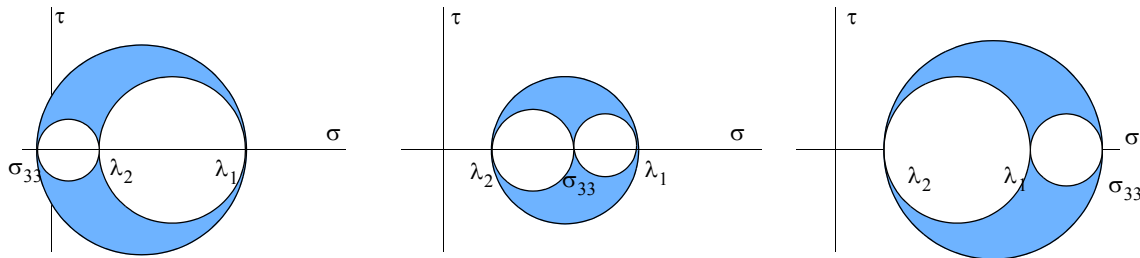


Figure 2.4. 3D Mohr's circles for planar stress states. Note that the locations of λ_1 and λ_2 are the same in all three plots. The peak shear stress depends on whether or not σ_{33} lies between the other eigenvalues.

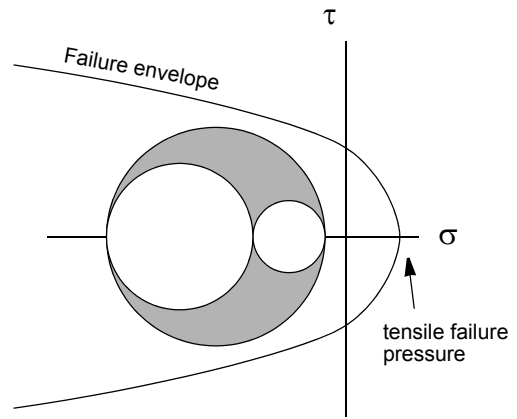
Exercise 7. The term “plane stress” is used if $\sigma_{i3}=0$ everywhere. In other words, only the upper 2×2 submatrix of the stress matrix can contain nonzero entries. Thus, σ_{33} is known implicitly to be zero. Use the 3D Mohr's circle to find the maximum shear stress for the following plane-stress states:

$$\begin{bmatrix} 43 & -24 \\ -24 & 57 \end{bmatrix}, \quad \begin{bmatrix} 2 & -36 \\ -36 & 23 \end{bmatrix}, \quad \begin{bmatrix} -73 & -36 \\ -36 & -52 \end{bmatrix}. \quad (2.71)$$

Answers: $3/2, 3/2, 2$

Engineering application of 3D Mohr's circle

The Coulomb-Mohr theory of failure postulates that there exists an “envelope” such that failure occurs when the (largest) Mohr's circle for the stress state reaches the envelope (in the simplest Mohr-Coulomb theory, the failure envelope is a straight line). The Mohr's circle for isotropic stress states degenerates to a single point on the σ -axis. Thus, failure under isotropic stress can occur only if the mean stress exceeds the tensile failure “pressure” where the failure envelope crosses the σ -axis. For less tensile or for compressive stress states, the Mohr's circle must have a nonzero radius in order to reach the failure envelope. In other words, sufficiently large shearing stresses must be present, the magnitude of which generally increases with increasing mean compression.



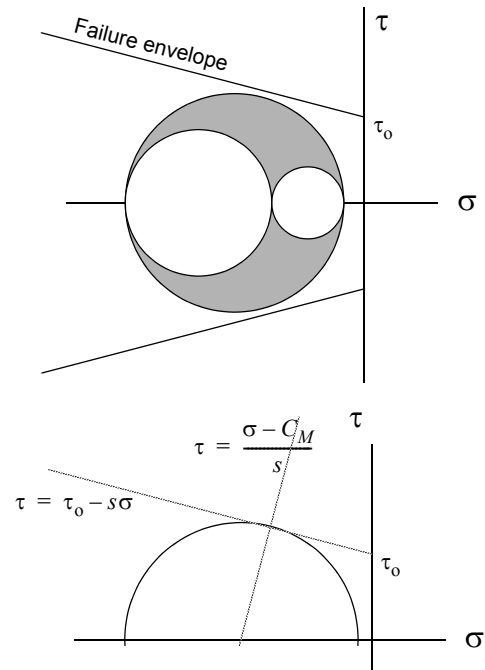
EXAMPLE 10. Consider a *linear* Mohr-Coulomb envelop:

$$\tau = \tau_0 - s\sigma, \quad (2.72)$$

where τ_0 and s are known material parameters. Express the Coulomb-Mohr failure criterion in terms of the center and radius of the largest Mohr's circle. Propose how the material parameters τ_0 and s may be measured in the laboratory.

Let C_M denote the center of the largest Mohr's circle. The line that passes through both the point of tangency and the center of the largest Mohr's circle is described by the equation

$$\tau = \frac{\sigma - C_M}{s}. \quad (2.73)$$



Solving the above two simultaneous equations shows that the failure tangency point is located at

$$\sigma_f = \frac{s\tau_o + C_M}{1 + s^2}. \quad (2.74)$$

$$\tau_f = \frac{\tau_o - sC_M}{1 + s^2}. \quad (2.75)$$

Therefore, the radius of Mohr's circle at the point of failure is

$$R_M = \sqrt{(\sigma_f - C_M)^2 + \tau_f^2}, \quad (2.76)$$

or, substituting from above,

$$R_M = \frac{\tau_o - sC_M}{\sqrt{s^2 + 1}}, \quad (2.77)$$

which is valid for $sC_M < \tau_o$ (i.e., before the envelop crosses the σ -axis).

Assuming $s \geq 0$, admissible (pre-failure) values for R_M and C_M satisfy

$$R_M < \frac{\tau_o - sC_M}{\sqrt{s^2 + 1}} \text{ and } C_M < \tau_o/s. \quad (2.78)$$

Note how the Mohr's circle radius at failure is linearly related to the center. In the laboratory, the material can be stressed to the point of failure for numerous stress states. The values of R_M and C_M just before the point of failure can be plotted, and a least squares linear fit to the data will provide an empirical curve

$$R_M = \alpha - \beta C_M. \quad (2.79)$$

Comparing this with Eq. (2.77) gives

$$s = \frac{\beta}{\sqrt{1 - \beta^2}} \text{ and } \tau_o = \frac{\alpha}{\sqrt{1 - \beta^2}}. \quad (2.80)$$

Distributional Mohr-Coulomb theory

Traditional Mohr-Coulomb theory states that material failure occurs at the instant the Mohr's circle touches the failure line. Microphysically, classic linear Mohr-Coulomb theory results if you consider an idealized body containing a large population of randomly oriented *same-sized* cracks. Any given crack will fail if the applied shear stress on the crack face is high enough to cause the matrix material near the crack edges to break. When all three principal stresses are compressive, but not equal, a crack will be subjected in general to both compressive normal stresses *and* shear stresses. Even though it shear stress plays the predominant role in shear crack failure, the existence of a normal compression is important because the resulting friction at crack faces helps reduce the amount of shear stress that must be suffered by the matrix material, thereby retarding failure. After working out the details, the presence of friction leads to a failure boundary in the Mohr diagram that is a straight line whose slope is determined by the coefficient of friction. If the friction is zero, the slope is zero and therefore the failure criterion reduces to Tresca theory.

Under traditional Mohr-Coulomb theory, material failure occurs at the instant the largest Mohr's circle reaches the failure line. However, an important implicit assumption of this criterion is that there actually *exists* a crack of the proper orientation that will map to that "kissing" (tangent) point.

Suppose there *isn't* a crack at the right orientation. Then the Mohr's circle can continue to expand beyond the failure line until, finally, a critical crack orientation (i.e., one that maps to a point on the failure line) is found. Dealing with this more realistic possibility requires speaking of *probabilities* that a super-critical crack orientation exists in your sample. We will assume that the cracks have uniformly random orientations. Since crack normals are unit vectors and unit vectors are points on the unit sphere, we are talking about a uniform distribution of points on the unit sphere.

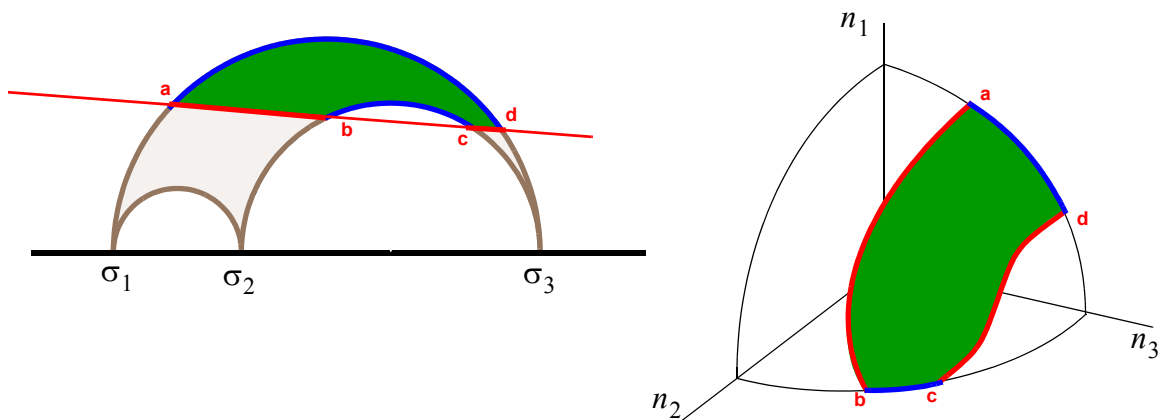


Figure 2.5. Points on the sphere map to points on the Mohr diagram and vice versa.

When all three principal stresses are distinct, each distinct point on an octant of the unit sphere maps to a distinct point on the Mohr diagram. The regions in the Mohr diagram that fall above the failure line [see Fig. 2.5(a)] are spawned from a region of crack orientations (defined by unit normal components $\{n_1, n_2, n_3\}$ which are regarded as points on the unit sphere) [see Fig. 2.5(b)].

Failure will occur if there exists any crack with an orientation in the shaded region on the spherical octant sketched in Fig. 2.5(b). Existence of a single failure line is based on an assumption that all crack sizes are equal. Reducing the crack size translates the failure line upward, and we will deal with that complication later. For now, let's consider the likelihood that a given *single* crack will fail. The only variable in this case is the crack's orientation. The probability of failure is the ratio of the shaded region on the octant to the total area of the octant. Of course, the probability of failure of a material sample depends on the total number of cracks in the sample — larger samples have more cracks, therefore increasing the likelihood that at least one of them will be critically oriented. The computation of failure probability is further complicated by the fact that, for real materials, the cracks are *not* all of the same size. Smaller cracks result in failure lines that are farther from the horizontal axis in the Mohr diagram, and they are therefore less likely to fail. Extremely tiny cracks will be entirely safe from failure regardless of their orientation because the outer Mohr's circle will be entirely below the failure line for such cracks. Thus, brittle failure truly is a “weakest link” theory.

To predict failure probabilities (accounting for distributed crack sizes, distributed crack orientations, and varying sample sizes) requires numerical methods for general stress states. However, considerable progress can be made by instead considering *triaxial* stress states. For triaxial loading, two eigenvalues are equal, and the third is distinct. A far better name for this type of loading would be “axisymmetric” because it implies a symmetry of stress about the eigenvector associated with the distinct eigenvalue. The normal and shear stresses on a plane are equal for all points on the unit sphere that are equidistant from this symmetry axis.

For triaxial loading, the 3D Mohr diagram *looks* a lot like a 2D Mohr diagram, but it isn't. For triaxial stress states, one of the inner circles in the 3D Mohr diagram degenerates to a single point (putting double eigenvalues there) while the other grows outward to actually overlap the outer circle. For triaxial states, there is no longer a one-to-one correspondence between points on the Mohr diagram and points on the sphere. This time, each point on the triaxial Mohr's circle is spawned by an infinite family of unit normals — namely all normals equidistant from the symmetry axis. To develop distributional Mohr-Coulomb theory for triaxial stress states, we are now seeking the finite “band” of unit normals that map to the *arc* of Mohr's circle that falls above the failure line.

Except when the failure line has a zero slope (Tresca theory), identifying this band of critical normals requires knowing if the triaxial stress state is triaxial compression (TXC), where the axial stress is more compressive than the lateral stresses, or triaxial extension (TXE), where the axial stress is less compressive than the lateral stresses. (Note: in laboratory experiments on brittle materials, all principal stresses are compressive and therefore the axial stress for TXE is *not* tensile — it is merely less compressive).

A TXC stress state can have the same Mohr's circle as a TXE state. The distinction is the location of the single root. For TXC, the distinct eigenvalue will be on the left (more compressive) side of the Mohr's circle and therefore, if the loading is observed so that the symmetry axis is vertical, the pole point will be on the left side of the Mohr circle. For

TXE, the pole point is on the right hand side. The pole point can be extremely useful for visualizing critical crack orientations. Specifically, you can center an image of the sphere at the pole point location appropriate to whether you are considering TXE or TXC. Recall that lines drawn from the pole point to locations on the Mohr diagram will have precisely the same orientation as the orientation of the unit normal that generated that normal-shear stress pair. Thus, because we have centered the image of the sphere at the pole point, any line drawn to the terminating points on the critical arc (i.e., the arc above the failure line) will intersect the sphere at precisely the terminating boundary of critical crack orientations. This graphical method for depicting the critical orientation band is illustrated in Fig. 2.6.

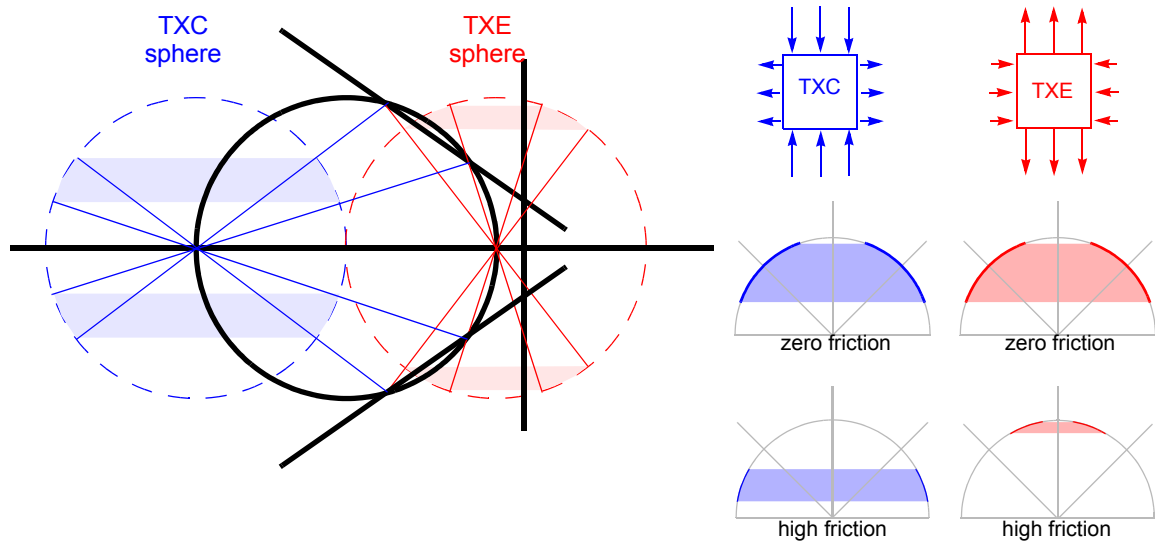


Figure 2.6. Graphical method for depicting critical orientation bands for triaxial loading.

The area of the critical bands on the sphere is proportional to band thickness when viewing the sphere from the side. For example, if the band thickness is $1/3$ of the sphere radius, then the band area on the spherical octant is $1/3$ of the total area of the octant, implying a failure probability of $1/3$. Note that the TXC bands in Fig. 2.6 are thicker than the TXE bands, which indicates that the triaxial compression state has more critical crack orientations and is therefore more likely to fail. At first, this result might seem to contradict the well-established fact that brittle materials are stronger (not *weaker*) under TXC than under TXE. However, this statement about the relative strengths in compression versus extension apply only when comparing triaxial stress *at the same pressure*. Pressure is the average of the stress eigenvalues. TXE has one extensional eigenvalue, but *two* compressive eigenvalues. When comparing TXE and TXC states that have *the same Mohr's circle*, the TXE state is actually less likely to fail because it is loaded under a more compressive mean stress than TXC. A more equitable comparison between TXE and TXC is shown in Fig. 2.7, where *different* Mohr's circles are used for TXE and TXC such that both stress states have the same pressure and equivalent shear (magnitude of the stress deviator). In this case, TXE is weaker than TXC, consistent with experimentally established fact.

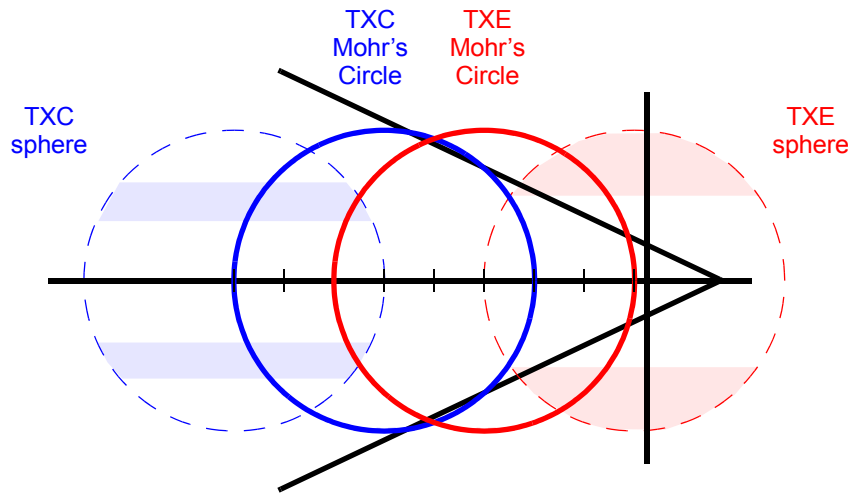


Figure 2.7. A comparison between TXC and TXE states that have the same pressure and equivalent shear stress.

Figure 2.7 graphically illustrates the probability that sample containing exactly one *single crack* will fail under TXC or TXE stress states, compared at the same pressure and equivalent shear (same Mohr's circle radius). The *quantitative* failure probabilities for a *single crack* are shown in Fig. 2.8 (one plot holds the magnitude of the stress deviator constant while varying the pressure; the other plot holds pressure constant while increasing the radius). Except for "apex stress states" (defined below) these plots again show that TXE states are more likely to fail than TXC. If the pressure is held fixed, and the Mohr's circle radius R is increased upward from zero, the first curve encountered is the TXE curve, which means that TXE is more likely to fail. Similarly, if the radius is held fixed while the pressure is decreased downward in magnitude from a perfectly safe "infinite" pressure (i.e., if the Mohr's circle of a given radius is translated from the far left in the Mohr diagram until it reaches the failure line), then TXE is the first stress state to begin having a nonzero probability of failure. The probability curves *cross* when the largest eigenvalue approaches the apex of the failure line (i.e., the point where the failure line crosses the horizontal axis). At these "apex" stress states, most of the critical arc of Mohr's circle is on tensile side of the circle and TXC becomes more likely to fail because TXC stresses (which have double eigenvalues on the right side of the Mohr's circle) actually have more tensile points on Mohr's circle than TXE.

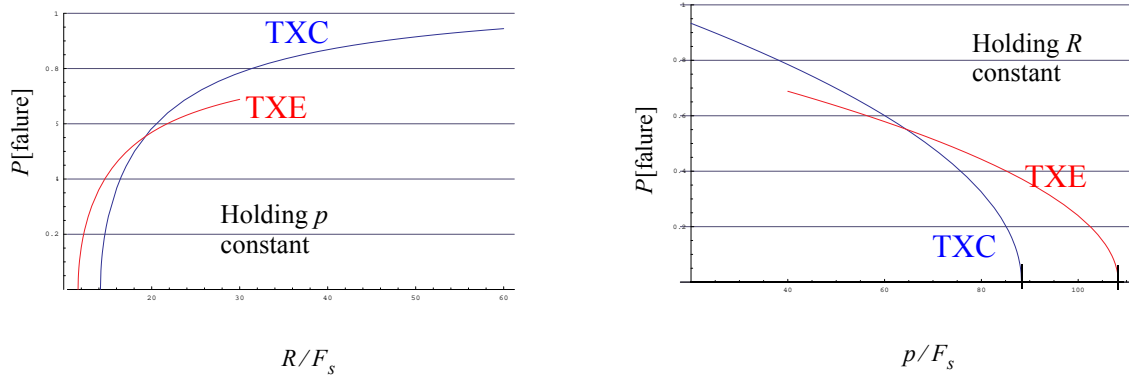


Figure 2.8. Failure probabilities for TXC and TXE stress states applied to a sample of material that contains exactly one crack. The scale factor F_s is the vertical intercept of the failure line, making it therefore equal to the shear failure stress for a crack loaded without friction at the crack faces.

When considering a sample with an increasing number of cracks, *but all of the same size*, the failure probability curves approach step functions, equivalent to classical Mohr-Coulomb theory. Real materials, however, do not have equal-sized cracks — they have a larger population of tiny (therefore subcritical) cracks and a relatively small population of “potentially dangerous” larger crack sizes. Figures 2.9, 2.10, and 2.11 illustrate the effect of accounting for crack size distribution. Interestingly, when allowing for multiple crack sizes, the cross-over phenomenon seen in Fig. 2.8 goes away. Recall that the cross-over occurs when the Mohr’s circle is near the failure line apex. Recall that a decrease in crack size corresponds to an upward translation of the failure line. Thus, since most of the cracks are small, a given a Mohr’s circle will be far away from most of the failure apex points.

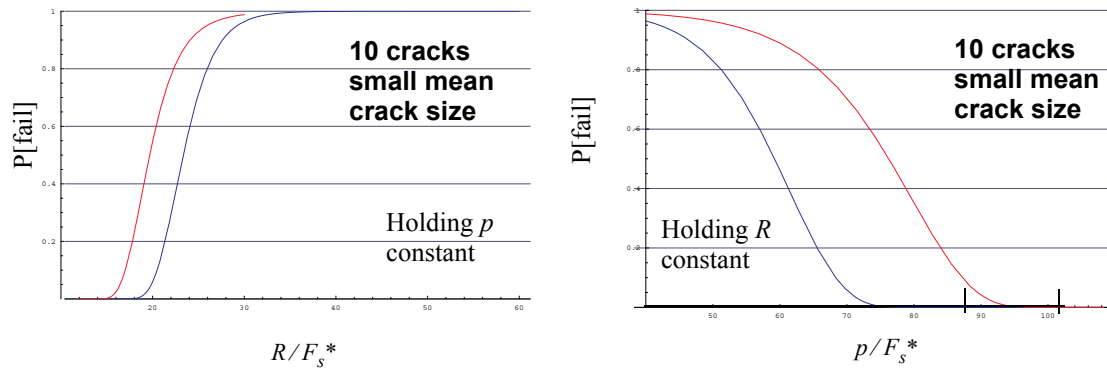


Figure 2.9. Probability that 10 exponentially sized cracks will fail. This plot corresponds to 10 cracks whose sizes are exponentially distributed with a mean crack size that is 150 times smaller than the single crack size used in the previous plot. Most of the cracks are subcritical. Only the larger cracks dominate the response. Thus, a spread in the data is generated reminiscent of the spread for a sample containing only a single crack. Crack size distribution, however, clearly affects the *shape* of the distribution, eliminating large slope changes at a Mohr-Coulomb threshold.

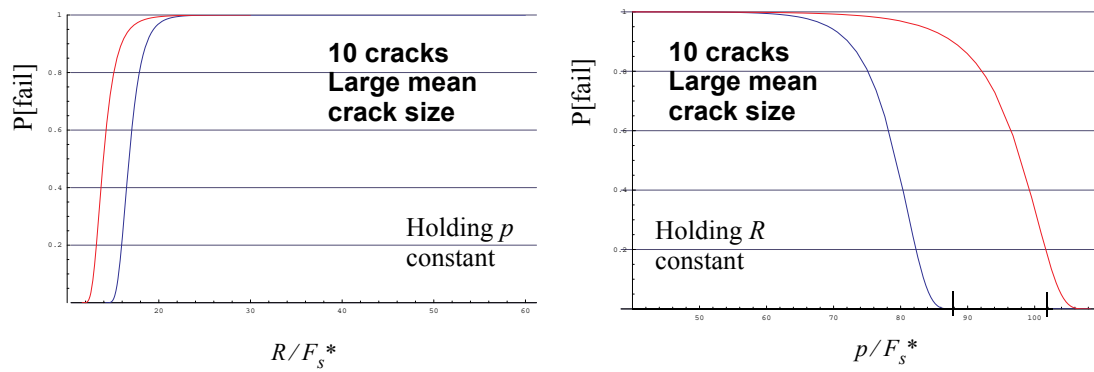


Figure 2.10. Probability that 10 exponentially sized but larger cracks will fail. This plot is equivalent to Fig. 2.9 except that the mean crack size is 10 times larger.

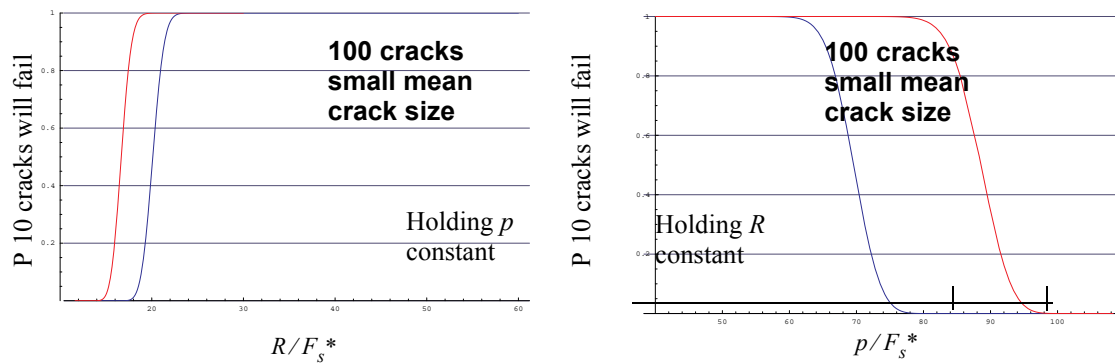
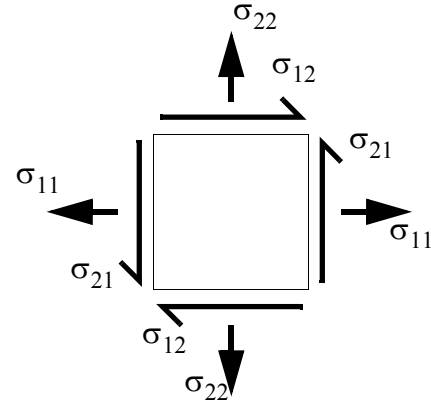


Figure 2.11. Effect of increasing the sample size. This plot is equivalent to Fig. 2.9 except that the sample 10 times as many cracks. This is like increasing the sample volume by a factor of 10.

3. Mohr's circle for nonsymmetric matrices

Mohr's circle for nonsymmetric matrices is very similar to that for symmetric matrices. The theory has been known for approximately 100 years, but very few people know about it, so (remarkably and sadly) the method continues to receive an audience in contemporary literature* when it really belongs in undergraduate math and engineering textbooks.

To draw Mohr's circle for a nonsymmetric matrix, you treat the matrix as though it represents a nonsymmetric stress. This time, however, the off diagonal stresses are no longer symmetric, so we must be careful to stay consistent with our symmetry conventions. For our examples, we will adopt the following convention



$$\sigma_{ij} \text{ is the } j^{\text{th}} \text{ component of traction on the } i^{\text{th}} \text{ face.} \quad (3.1)$$

This means that the traction vector on a face with normal \mathbf{n} is given by

$$t_i = \sum_{j=1}^3 \sigma_{ij} n_j. \quad (3.2)$$

Many authors define the stress tensor as the transpose of this definition. This should present very little difficulty because all that's really important is drawing the stress element correctly. With our definition, the traction on the i^{th} -face is given by the i^{th} COLUMN of the stress matrix.†

Consider a generic nonsymmetric 2×2 matrix:

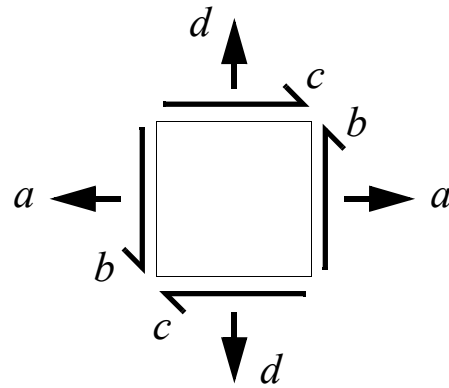
$$\begin{bmatrix} a & c \\ b & d \end{bmatrix}. \quad (3.3)$$

* See, for example,

Treagus, S. (1995), Superposed deformations by Mohr construction.

† with the other definition, it is the i^{th} row. Regardless of the definition, just take care to draw the final stress element correctly.

For constructing Mohr's circle, it is again useful to "pretend" that the matrix is a stress state where $\sigma_{11} = a$, $\sigma_{21} = b$, $\sigma_{12} = c$, and $\sigma_{22} = d$. This stress state is sketched at right.



To construct Mohr's circle, you examine the normal and shear stresses on each face to construct a pair of numbers for each face.

The face with the horizontal normal will again be called the "H" face. The face with the vertical normal will be the "V" face. For the stress state shown, the normal stress on the H-face equals a , and the normal stress on the V-face equals d . By the left hand rule, the shearing stress on the H-face is $-b$ and the shearing stress on the V-face is c .



Figure 3.1. The H and V faces of the "stress" element. The outward normal of the H face is horizontal and the outward normal of the V face is vertical.

Mohr diagram for nonsymmetric matrices

We again seek a method of computing the normal and shear stresses on a plane whose normal makes an angle θ with the horizontal. Again, we define the normal "stress" σ to be positive if it is tensile. The numerical sign for the shearing stress τ is assigned by a *left-hand rule*.

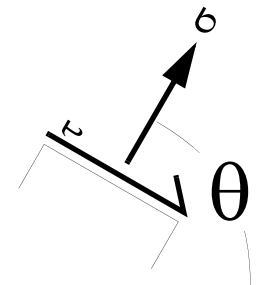


Figure 3.2. Sign convention for normal and shearing "stress" on a plane.

The normal and shearing stresses depend on the orientation of the plane. In particular, comparing Fig. 3.1 with Fig. 3.2, we observe that

$$\begin{aligned}
 \text{H-face } (\theta = 0): \quad & \sigma = \sigma_{11} = a \quad \text{and} \\
 & \tau = -\sigma_{21} = -b \\
 \text{V-face } (\theta = \frac{\pi}{2}): \quad & \sigma = \sigma_{22} = d \quad \text{and} \quad \tau = +\sigma_{12} = +c. \quad (3.4)
 \end{aligned}$$

Drawing the nonsymmetric stress element does give you a more physical sense of the matrix components in the sense that they correspond to traction vectors on the stress element faces. However, you can always just skip drawing the element by noting the direct correspondence between the original 2×2 matrix and the H and V coordinates. Namely:

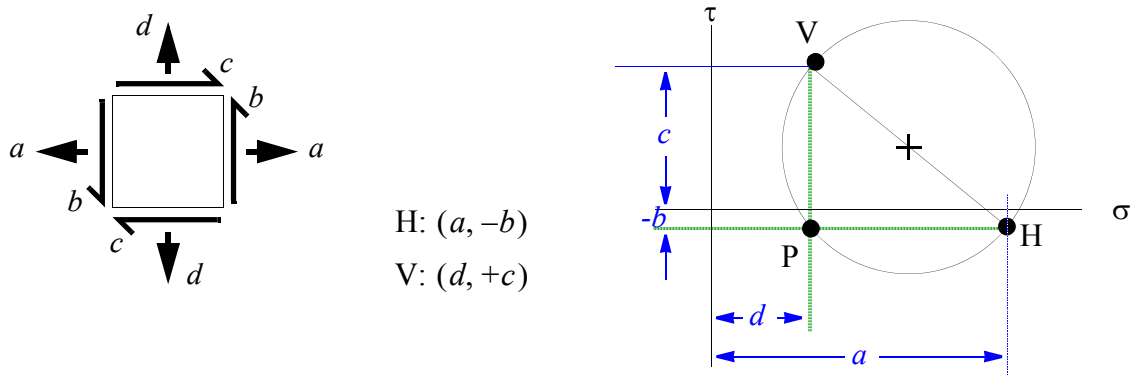
$$\begin{bmatrix} \sigma_{11} & \sigma_{12} \\ \sigma_{21} & \sigma_{22} \end{bmatrix} = \begin{bmatrix} H_1 & V_2 \\ -H_2 & V_1 \end{bmatrix}. \quad (3.5)$$

We are interested in the values of σ and τ on a plane of arbitrary orientation θ . These normal and shear “stresses” vary with θ . We again imagine a graph in which the shearing stress $\tau(\theta)$ is plotted parametrically against the corresponding normal stress $\sigma(\theta)$ for various values of the orientation angle θ . It is proved in the Appendix that this closed path must be a *circle*, which is called Mohr's circle.

The H-face corresponds to $\theta=0$. Hence Eq. (2.3) tells us that Mohr's circle must pass through the point $(a, -b)$ when $\theta=0$. It must also pass through the point (d, c) when $\theta=\pi/2$. Consequently, we have deduced two points that must lie on the circle. The Appendix provides a proof of that the following very important property holds even for nonsymmetric Mohr's circles:

Whenever the orientations of two planes differ by exactly 90 degrees, the corresponding points on Mohr's circle will be diametrically opposite each other.

Consequently, not only are the points H and V on Mohr's circle, they are also opposite sides of the circle! This added restriction uniquely defines the Mohr's circle. To construct Mohr's circle, simply plot H and V, and then draw a circle such that the line connecting H and V is a major diameter of the circle. The pole point P is constructed in the familiar way (by intersecting a horizontal line through H with a vertical line through V).



The Mohr's circle for nonsymmetric matrices is no longer symmetric about the σ -axis! As before, the principal values of the matrix correspond to the values of σ where the shear stress is zero. For symmetric matrices, there were always two such points because the Mohr's circle was symmetric about the σ -axis. For nonsymmetric matrices, the Mohr's circle might not cross the σ -axis at all! In that case, the two eigenvalues are complex. Very kool, eh?

Mohr's circle for an anti-symmetric matrix

Consider the most general form for an anti-symmetric 2×2 matrix:

$$\begin{bmatrix} 0 & \gamma \\ -\gamma & 0 \end{bmatrix}. \quad (3.6)$$

Applying Eq. (3.5), we write

$$\begin{bmatrix} 0 & \gamma \\ -\gamma & 0 \end{bmatrix} = \begin{bmatrix} H_1 & V_2 \\ -H_2 & V_1 \end{bmatrix}, \quad (3.7)$$

and therefore conclude that the H and V points are

$$\begin{aligned} H: (0, \gamma) \\ V: (0, \gamma). \end{aligned} \quad (3.8)$$

This shows that the Mohr's circle for any anti-symmetric matrix degenerates to a single point a distance γ on the τ axis. This is an interesting result because it shows that all anti-symmetric 2×2 matrices are isotropic in the sense that their components are unaffected by a rotation in the plane.

Mohr's circle for the symmetric and skew symmetric parts

Consider a general matrix

$$\begin{bmatrix} a & c \\ b & d \end{bmatrix}. \quad (3.9)$$

The symmetric part of this matrix is

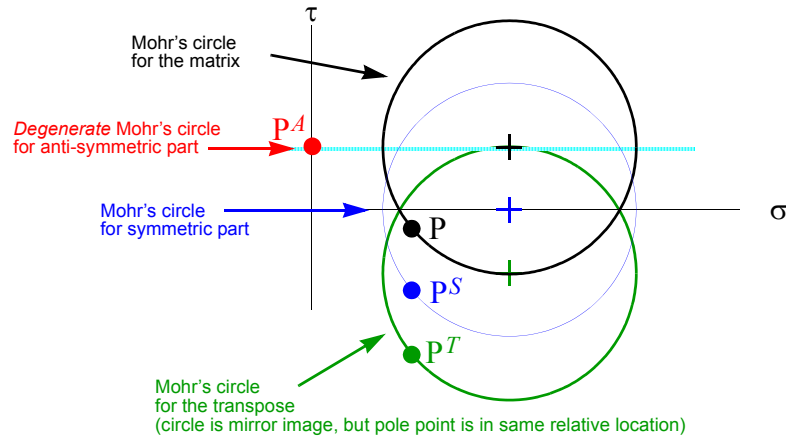
$$\begin{bmatrix} a & \frac{c+b}{2} \\ \frac{c+b}{2} & d \end{bmatrix}. \quad (3.10)$$

The anti-symmetric part of the matrix is

$$\begin{bmatrix} 0 & \frac{c-b}{2} \\ \frac{b-c}{2} & 0 \end{bmatrix}. \quad (3.11)$$

The corresponding Mohr's circles are shown below, where the pole points for the original matrix, its transpose, the symmetric part, and the anti-symmetric part are labeled P, P^T , P^S , and P^A , respectively.* The Mohr's circle for the transpose is the mirror image of the Mohr's circle for the original matrix, but the pole point for the transpose is in the same rel-

ative location — not the mirror image! Mohr's circle for the symmetric part of the matrix is obtained by simply shifting the Mohr's circle for the original matrix until it is symmetric about the σ -axis. The anti-symmetric Mohr's circle is a degenerate point at the same height as the center of the original Mohr's circle.



* Keep in mind: Mohr's circle is virtually useless without knowing the location of the H and V points — these points are needed to construct the component matrices with respect to the laboratory basis. To keep our drawings cleaner, we have plotted only P, not H and V. However, the location of P is sufficient to give you the H and V points because you can draw a horizontal line through P to obtain H and a vertical line through P to obtain V.

Eigenvalues and eigenvectors of nonsymmetric matrices

As before, an eigenvector is the normal to a plane where the shear stress is zero. The eigenvalue is the normal component of traction on that plane. Stated mathematically, a “right” eigenvector of a matrix $[B]$ is any vector $\{u\}$ for which

$$[B]\{u\} = \lambda\{u\}. \quad (3.12)$$

The scalar λ is the associated eigenvalue. Rearranging the above definition,

$$([B] - \lambda[I])\{u\} = \{0\}. \quad (3.13)$$

This condition is possible only if the determinant of $[B] - \lambda[I]$ is zero. Applying this restriction gives the “characteristic” equation for the eigenvalues:

$$\begin{aligned} \lambda^2 - I_1\lambda + I_2 &= 0, \\ \text{where } I_1 &= \text{tr}[B] = B_{11} + B_{22} \\ \text{and } I_2 &= \det[B] = B_{11}B_{22} - B_{12}B_{21}. \end{aligned} \quad (3.14)$$

Eigenvectors corresponding to *distinct* eigenvalues are always linearly independent. Eq. (3.14) is quadratic, so there is a possibility that the eigenvalue has an algebraic multiplicity of two (*i.e.*, it is a double root). When an eigenvalue has an algebraic multiplicity greater than one, then there is *at least* one associated eigenvector, but the geometric multiplicity (*i.e.*, the number of linearly independent eigenvectors associated with the eigenvalue) is always less than or equal to the algebraic multiplicity.

A “left” eigenvector of the matrix $[B]$ is any vector $\{w\}$ for which

$$\{w\}[B] = \lambda\{w\}. \quad (3.15)$$

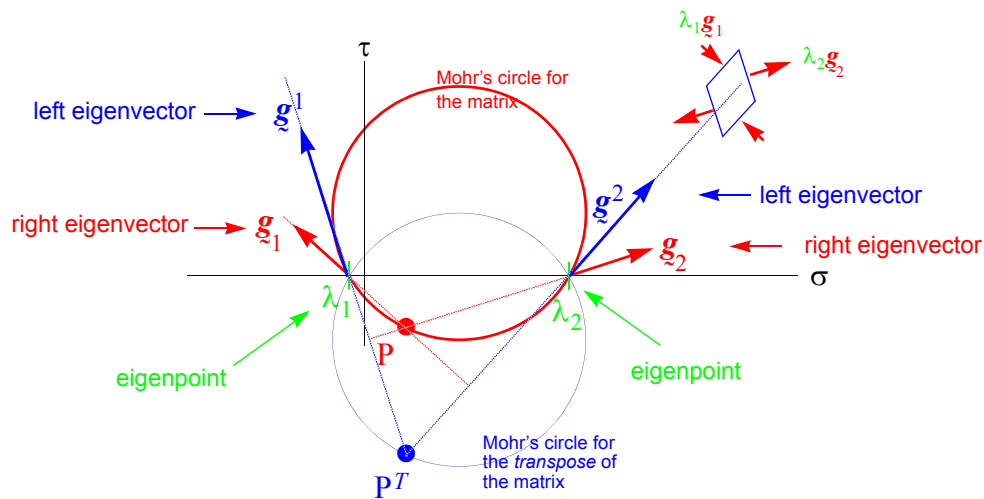
The above equation can be written

$$[B]^T\{w\} = \lambda\{w\}. \quad (3.16)$$

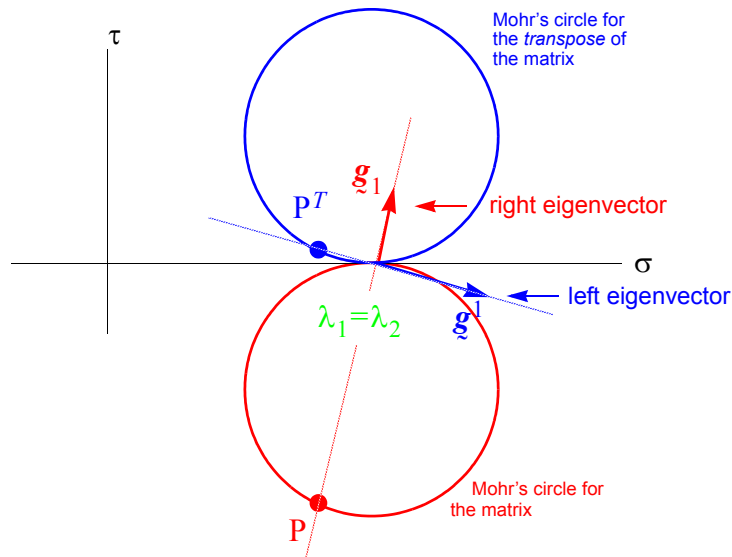
Consequently, the left-eigenvectors of $[B]$ are identical to the *right*-eigenvectors of the transpose matrix $[B]^T$. The trace and determinant of $[B]^T$ are equal to the trace and determinant of $[B]$. Consequently, the characteristic equations — and hence the eigenvalues — are the same for both the right and left eigenproblems. The distinction between left and right eigenvectors is necessary only for nonsymmetric matrices.

For *symmetric* matrices, recall that the Mohr's circle is always symmetric about the σ -axis, so the Mohr's circle for a symmetric matrix always has two points — called “**eigenpoints**” — at which $\tau=0$. The eigenvalues equal the values of σ at these two eigenpoints. The eigenvalues are always real for symmetric matrices. Each eigenvector corresponding to a particular eigenvalue is in the same direction as the line from the pole point to the appropriate eigenpoint. For symmetric matrices, the two eigenpoints are always diametrically opposite each other on Mohr's circle. Recall that diametrically opposite points always correspond to mutually perpendicular planes. Consequently, for symmetric matrices, the eigenvectors are always mutually perpendicular (or may be so chosen if the matrix is isotropic).

For nonsymmetric matrices, an eigenvalue is again defined to be the value of σ at an eigenpoint (*i.e.*, a point on Mohr's circle where $\tau=0$). Note, however, that the Mohr's circle might be so far distant from the σ -axis that there aren't *any* points on the circle where $\tau=0$. In this case, there are no real eigenpoints and the eigenvalues are complex-conjugate numbers. If the Mohr's circle is just barely tangent to the σ -axis, then the eigenvalues have an algebraic multiplicity of two and a geometric multiplicity of one. If the Mohr's circle crosses the σ -axis, then the normal stresses at the two crossing points (the eigenpoints) are equal to the eigenvalues. Lines from the pole point to the two eigenpoints give the right eigenvectors. The lines from the *transpose* pole point to the crossing points give the *left* eigenvectors. For nonsymmetric matrices, the eigenvectors are generally *not* mutually perpendicular. Consequently, illustrating the eigenvectors requires a stress element in the shape of a parallelogram with sides formed by the *left* eigenvectors (aargh!).



For nonsymmetric matrices, there's no guarantee that there will be two eigenvectors. Sometimes there's only one. This occurs when the Mohr's circle just "kisses" the σ -axis as shown below:



Exercise 8. Use Mohr's circle to find a 2×2 matrix having *all nonzero components* but having both eigenvalues equal to zero. *Hint: you desire a zero eigenvalue of multiplicity 2, so you must construct a nonsymmetric matrix whose Mohr's circle just "kisses" the point $(0,0)$. Draw any convenient circle that fits this description and select any two diametrically opposite points on this circle to be your H and V points (make sure you select points having nonzero coordinates). From there, draw the "stress" element and construct the matrix.*

EXAMPLE 11. Characterize the set of all possible "square roots" of the 2×2 identity matrix.

SOLUTION:

We seek restrictions on $\{a, b, c, d\}$ such that

$$\begin{bmatrix} a & c \\ b & d \end{bmatrix} \begin{bmatrix} a & c \\ b & d \end{bmatrix} = \begin{bmatrix} 1 & 0 \\ 0 & 1 \end{bmatrix}. \tag{3.17}$$

Multiplying this out, we find that

$$\begin{aligned}a^2 + cb &= 1, \\d^2 + cb &= 1 \\b(a + d) &= 0 \\c(a + d) &= 0.\end{aligned}\tag{3.18}$$

Analyzing these restrictions shows that the “square root” of the 2×2 identity matrix must fall into one of the following two categories:

$$a + d \neq 0, \text{ in which case the solution is } \pm \begin{bmatrix} 1 & 0 \\ 0 & 1 \end{bmatrix}\tag{3.19}$$

$$a + d = 0, \text{ in which case the solution is } \pm \begin{bmatrix} \sqrt{1 - cb} & c \\ b & -\sqrt{1 - cb} \end{bmatrix},\tag{3.20}$$

where c and b are arbitrary. The first solution corresponds to the diagonal components being equal to each other, in which case, the off-diagonals must be zero. The second solution corresponds to the diagonal components being negatives of each other. An eigenvalue analysis of this latter solution shows that, regardless of the values of c and b , the eigenvalues of the matrix in Eq. (3.20) must equal $+1$ and -1 . Conversely, any matrix whose eigenvalues are $+1$ and -1 is expressible in the form (3.20).

The two Mohr's circles corresponding to Eq. (3.19) are simply the degenerate zero-radius circles at the points $(1,0)$ and $(-1,0)$. The more interesting *infinite family* of Mohr's circles corresponding to Eq. (3.20) is the set of any and all circles that pass through the points $(1,0)$ and $(-1,0)$.

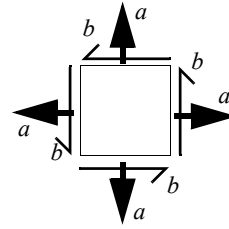
Exercise 9. Construct some nonsymmetric real “square roots” of the identity matrix and show their Mohr's circles.

Exercise 10. Prove that the matrix $\begin{bmatrix} 2 & -1 \\ 4 & -2 \end{bmatrix}$ is a “square root” of the ZERO matrix, and draw its Mohr's circle.

Does the Mohr's circle have any similarities to the one you constructed for Exercise 8?

EXAMPLE 12. Back in Example 3, we looked at an isotropic *symmetric* 2×2 matrix. For 2-dimensional matrices, there also exist *nonsymmetric* isotropic matrices. The most general form of an isotropic 2×2 matrix is

$$\begin{bmatrix} a & -b \\ b & a \end{bmatrix}, \quad (3.21)$$



where a and b are scalars. The interpretation of such a matrix becomes more clear if we instead represent the scalars in terms of a change of variables, ρ and α such that

$$a = \rho \cos \alpha \quad \text{and} \quad b = \rho \sin \alpha. \quad (3.22)$$

Then Eq. (3.21) can be written

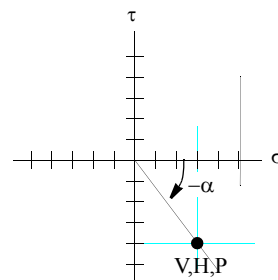
$$\rho \begin{bmatrix} \cos \alpha & -\sin \alpha \\ \sin \alpha & \cos \alpha \end{bmatrix}. \quad (3.23)$$

In this form, we recognize the matrix as a scalar multiple of a rotation matrix. The H and V points are identical:

$$\begin{aligned} \text{H: } & (r \cos \alpha, -r \sin \alpha) \\ \text{V: } & (r \cos \alpha, -r \sin \alpha). \end{aligned} \quad (3.24)$$

The H and V points will always be identical for any isotropic matrix. Conversely, if the H and V points coincide, then the matrix must be isotropic.

Mohr's circle for an isotropic matrix degenerates to a single point. This means that, no matter how you look at this stress state, the matrix that represents it will always be the same. The components will not change upon an orthogonal change of basis. The degenerate isotropic Mohr's circle will lie off the symmetric axis whenever the matrix is nonsymmetric (*i.e.*, whenever $\alpha \neq 0$). Consequently, nonsymmetric isotropic matrices have no real 2×2 eigenvalues.



Exercise 11. Demonstrate that the following matrix is isotropic by showing that its Mohr's circle degenerates to a single point:

$$\begin{bmatrix} 3 & 4 \\ -4 & 3 \end{bmatrix}. \quad (3.25)$$

EXAMPLE 13. Consider the most general form for a 2×2 in-plane rotation matrix:

$$\begin{bmatrix} \cos \theta & -\sin \theta \\ \sin \theta & \cos \theta \end{bmatrix}. \quad (3.26)$$

The H and V points are

$$\begin{aligned} \text{H: } & (\cos \theta, -\sin \theta) \\ \text{V: } & (\cos \theta, -\sin \theta). \end{aligned} \quad (3.27)$$

This shows that the Mohr's circle for any rotation matrix degenerates to a *single point* that lies a unit distance from the origin. Thus a 2×2 in-plane rotation matrix is isotropic with respect to any in-plane change of basis. The rotation angle is the negative of the angular position of the (degenerate) Mohr's circle.

Mohr's circle for the polar decomposition

Consider a general matrix

$$F = \begin{bmatrix} F_{11} & F_{12} \\ F_{21} & F_{22} \end{bmatrix}. \quad (3.28)$$

Assuming this matrix is invertible and has a positive determinant, the polar decomposition is defined

$$F = RU = VR, \quad (3.29)$$

where R is a rotation matrix of the form of Eq. (3.26) and $[V]$ and $[U]$ are symmetric positive definite matrices. The decomposition is unique.

For 3×3 matrices, the general method for determining a polar decomposition requires an eigenvalue analysis. However, for 2×2 matrices, the decomposition can be performed rapidly by the following formula:

$$R = \begin{bmatrix} \cos\theta & -\sin\theta \\ \sin\theta & \cos\theta \end{bmatrix}, \quad (3.30)$$

where

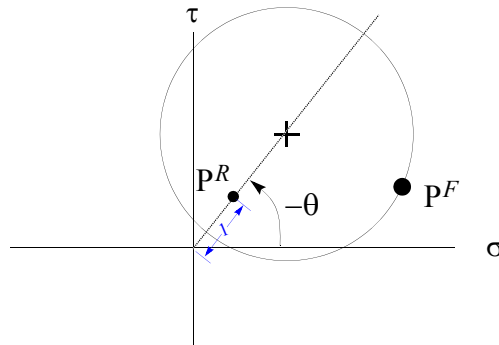
$$\begin{aligned} \cos\theta &= \frac{F_{11} + F_{22}}{\sqrt{(F_{11} + F_{22})^2 + (F_{21} - F_{12})^2}} \\ \sin\theta &= \frac{F_{21} - F_{12}}{\sqrt{(F_{11} + F_{22})^2 + (F_{21} - F_{12})^2}}. \end{aligned} \quad (3.31)$$

Beware! You must define $\cos\theta$ and $\sin\theta$ *separately* in order to uniquely determine the rotation angle. It is certainly true that

$$\tan\theta = (F_{21} - F_{12}) / (F_{11} + F_{22}), \quad (3.32)$$

but you must never use this relation to define the rotation angle because there are always *two* angles θ in the range from 0 to 2π that satisfy the above equation. By contrast there is only one angle in the range from 0 to 2π that satisfies Eq. (3.31). The rotation angle θ is measured counterclockwise.

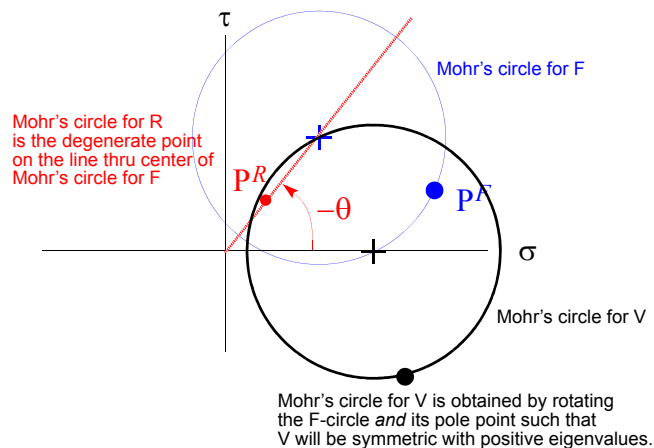
The Mohr's circle for the rotation matrix is degenerate and it will always be located at a unit distance from the origin on a line that passes through the center of the Mohr's circle for the original matrix F . In other words, the rotation angle is the negative of the angle to the center of Mohr's circle for F .



Once the rotation matrix R is known, the polar stretches may be computed by

$$U = R^T F \quad \text{and} \quad V = F R^T. \quad (3.33)$$

The Mohr's circle for the left stretch $[V]$ is the Mohr's circle that would be obtained by rotating the Mohr's circle for $[F]$ until it is symmetric about the σ axis. To satisfy the restriction that $[V]$ be positive definite, the rotation must be such that both eigenvalues of $[V]$ will be positive. The pole point for $[V]$ is obtained by similarly rotating the pole point for $[F]$. Thus, corresponding to the above sketch, we have.

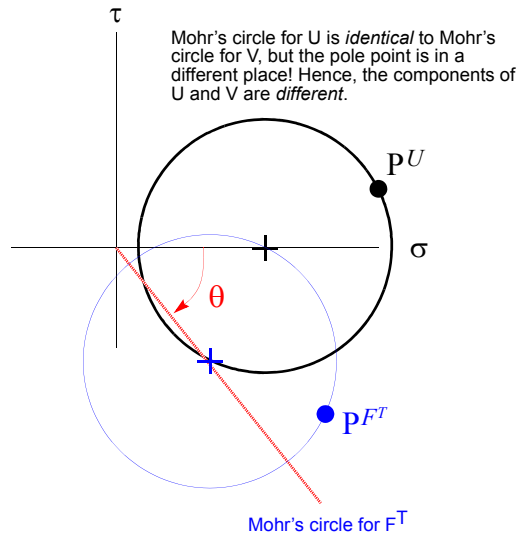


Of course, if your intent is to obtain a quick graphical estimate of the polar stretch, this figure could be obtained by merely rotating your sheet of paper by an amount equal to the rotation angle.

The Mohr's circle for the right stretch $[U]$ is identical to that for $[V]$. The only difference is where the pole point is located. Probably the simplest way to locate the pole point is to recognize that

$$F^T = U R^T. \quad (3.34)$$

Hence, the right stretch for $[F]$ is the left stretch for $[F^T]$. The following figure shows the Mohr's circle for $[F^T]$ and the corresponding pole point for $[U]$:



EXAMPLE 14. Consider the following deformation gradient matrix:

$$[F] = \begin{bmatrix} -1 & -2 \\ 3 & 4 \end{bmatrix}. \tag{3.35}$$

- (a) Determine the polar decomposition analytically.
- (b) Determine the polar decomposition graphically using Mohr's circle.

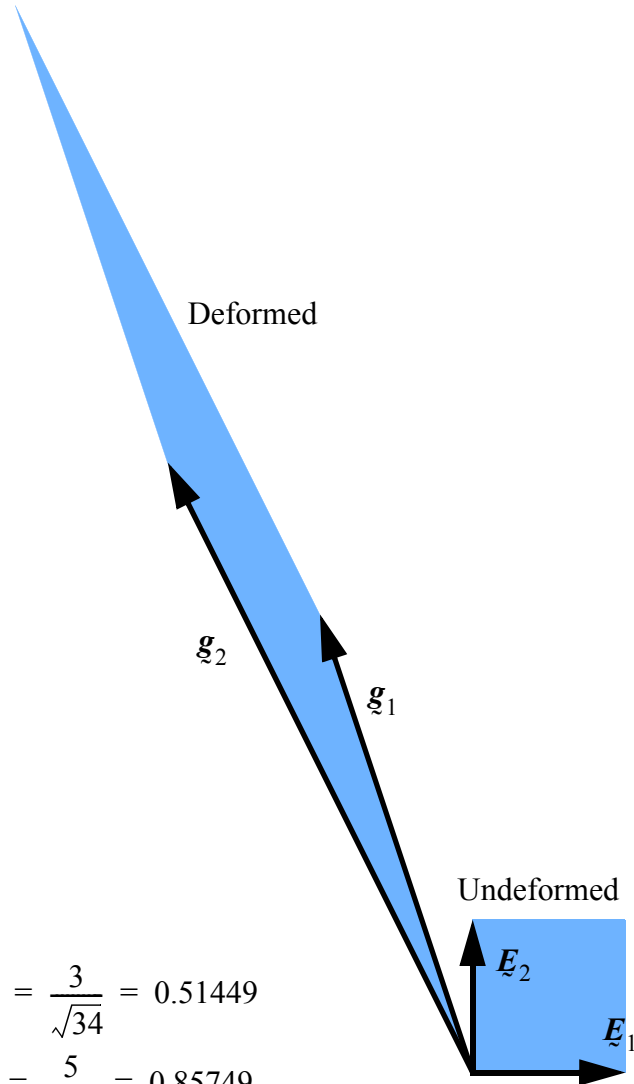
SOLUTION (PART A):

Before starting an analytical solution, it is useful to first sketch the deformation associated with the deformation gradient tensor. Specifically, consider a unit square whose sides are formed by the laboratory basis $\{\underline{E}_1, \underline{E}_2\}$. Under the above deformation this square deforms to a parallelogram having sides defined by two vectors $\underline{g}_1 = \underline{F} \cdot \underline{E}_1$ and $\underline{g}_2 = \underline{F} \cdot \underline{E}_2$. In other words, the material originally aligned with $\underline{E}_1 = \{1, 0\}$ deforms to a new vector given by the first column of $[F]$, namely $\{\underline{g}_1\} = \{-1, 3\}$. Similarly, the material originally aligned with $\underline{E}_2 = \{0, 1\}$ deforms to $\{\underline{g}_2\} = \{-2, 4\}$. This deformation is sketched at right.

Note that $\det[F] = 2$, showing that $[F]$ is invertible with a positive determinant. This is also consistent with our sketch since the area does appear to have doubled. For the rotation angle, Eq. (3.31) gives

$$\begin{aligned} \cos\theta &= \frac{-1 + 4}{\sqrt{(-1 + 4)^2 + (3 + 2)^2}} = \frac{3}{\sqrt{34}} = 0.51449 \\ \sin\theta &= \frac{3 + 2}{\sqrt{(-1 + 4)^2 + (3 + 2)^2}} = \frac{5}{\sqrt{34}} = 0.85749 \end{aligned} \tag{3.36}$$

Hence, the rotation angle is 59.04° measured counter-clockwise. Applying Eq. (3.30) gives the polar rotation matrix:



$$R = \begin{bmatrix} \cos\theta & -\sin\theta \\ \sin\theta & \cos\theta \end{bmatrix} = \frac{1}{\sqrt{34}} \begin{bmatrix} 3 & -5 \\ 5 & 3 \end{bmatrix} = \begin{bmatrix} 0.51449 & -0.85749 \\ 0.85749 & 0.51449 \end{bmatrix}. \quad (3.37)$$

Applying Eq. (3.33) gives the polar stretches:

$$U = R^T F = \frac{1}{\sqrt{34}} \begin{bmatrix} 3 & 5 \\ -5 & 3 \end{bmatrix} \begin{bmatrix} -1 & -2 \\ 3 & 4 \end{bmatrix} = \frac{1}{\sqrt{34}} \begin{bmatrix} 12 & 14 \\ 14 & 22 \end{bmatrix} = \begin{bmatrix} 2.058 & 2.401 \\ 2.401 & 3.773 \end{bmatrix} \quad (3.38)$$

$$V = F R^T = \frac{1}{\sqrt{34}} \begin{bmatrix} -1 & -2 \\ 3 & 4 \end{bmatrix} \begin{bmatrix} 3 & 5 \\ -5 & 3 \end{bmatrix} = \frac{1}{\sqrt{34}} \begin{bmatrix} 7 & -11 \\ -11 & 27 \end{bmatrix} = \begin{bmatrix} 1.200 & -1.886 \\ -1.886 & 4.630 \end{bmatrix}. \quad (3.39)$$

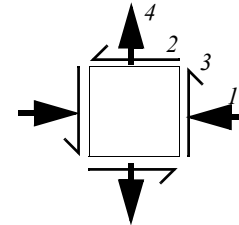
This completes the analytical derivation of the polar decomposition. One simple check that you can do is to simply verify that the determinants of $[U]$ and $[V]$ are both equal to the determinant of $[F]$. Even if you only want the analytical result, it is always a good idea to go ahead and do the Mohr's circle as a double check on your work, which leads into part (b) of this problem.

SOLUTION (PART B):

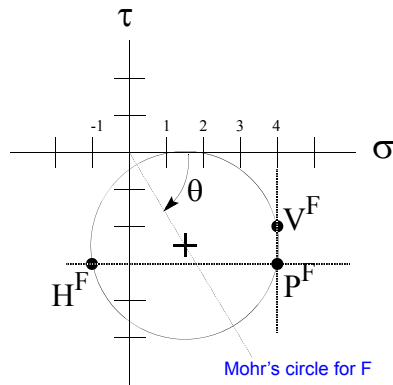
For Mohr's circle, we pretend that the matrix for $[F]$ is a stress matrix as shown at right. The H- and V-points for the $[F]$ matrix are:

$$H:(-1,-3) \quad (3.40)$$

$$V:(4,-2). \quad (3.41)$$



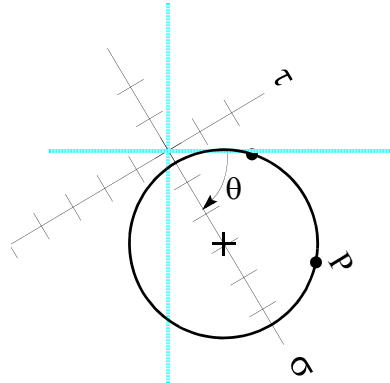
The corresponding Mohr's circle is:



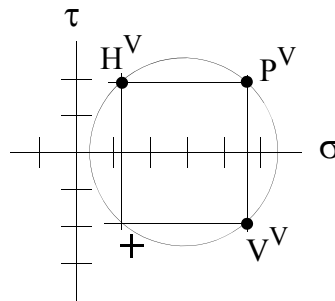
It's just a coincidence that this Mohr's circle happens to just barely "kiss" the σ -axis.

The polar rotation angle θ is, by convention, always measured counterclockwise from the laboratory horizontal. The rotation angle is the *negative* of the angle to the center of the Mohr's circle when this angle is measured counterclockwise. The center of the circle is at the point $(1.5, -2.5)$ therefore the rotation angle is $\theta = 59.04^\circ$, which agrees with our result from part (a) and can be visually verified by inspection of Mohr's circle. The sign of the rotation angle is positive because the angle to the center of Mohr's circle is negative when measured counterclockwise.

To obtain the Mohr's circle for the left stretch $[V]$, we must rotate the Mohr's circle for $[F]$ until it is symmetric about the positive side of the σ -axis. Alternatively, we can leave the Mohr's circle for $[F]$ alone and instead rotate the σ - τ axes. The result is:



Importantly, the pole point remains unchanged during the rotation. If we draw this above picture in the familiar orientation where the σ -axis is horizontal, the result is:



In the above drawing, we have labeled the H and V points for the left stretch matrix $[V]$. We are interested in a graphical verification of our analytical results from part (a). Reading directly from the coordinate grid, the coordinates of the H and V points appear to be approximately

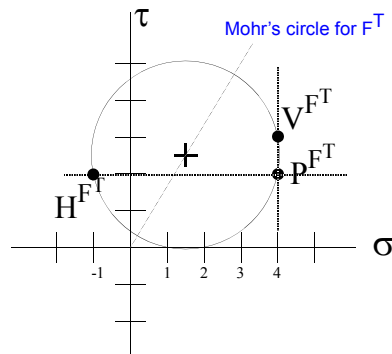
$$\begin{aligned} H^V &: (1.2, 1.9) \\ V^V &: (4.6, -1.9). \end{aligned} \tag{3.42}$$

Hence, the matrix for $[V]$ is

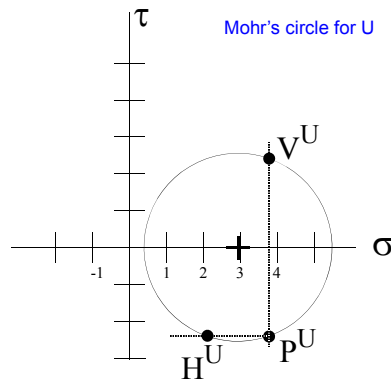
$$[V] = \begin{bmatrix} 1.2 & -1.9 \\ -1.9 & 4.6 \end{bmatrix}, \tag{3.43}$$

which agrees with the analytical result of Eq. (3.39).

Finding the right-stretch $[U]$ requires that we first construct the Mohr's circle for $[F]^T$. Keep in mind that the Mohr's circle for the transpose is the mirror image of the circle for the original matrix, but the pole point is in the same relative location!



The Mohr's circle for $[U]$ is obtained by rotating the Mohr's circle for $[F]$ and its pole point until it the rotated circle is symmetric about the positive σ -axis. Pass a horizontal line through the rotated pole point to obtain the H-point for $[U]$; pass a vertical line through the pole point to obtain the V-point. The resulting circle is identical to the Mohr's circle for $[V]$, but the pole point is in different location.



Reading coordinates off of the above figure, the approximate locations of the H and V-points for $[U]$ are

$$\begin{aligned} H^U: & (2.1, -2.4) \\ V^U: & (3.8, 2.4), \end{aligned} \tag{3.44}$$

from which the matrix for $[U]$ is constructed:

$$[U] = \begin{bmatrix} 2.1 & -2.4 \\ 2.4 & 3.8 \end{bmatrix}, \tag{3.45}$$

which agrees with Eq. (3.38).

Exercise 12. The deformation gradient matrix for simple shear is of the form

$$\begin{bmatrix} 1 & kt \\ 0 & 1 \end{bmatrix}, \quad (3.46)$$

where k is a constant and t is time. Chose a value for k and sketch the Mohr's circles at a representative number of times.

Exercise 13. (a) Construct a deformation gradient matrix $[F]$ for which the rotation angle is 120° and the left stretch tensor is given by $[V] = \begin{bmatrix} 10 & 4 \\ 4 & 4 \end{bmatrix}$.

(b) Solve the inverse problem [as was done in part (b) of Example 14] to *graphically* determine $[R]$ and $[V]$ and $[U]$, starting with the matrix for $[F]$. *Do not use formulas; the term "graphically" means you must make accurate drawings and measure coordinates and angles with rulers and protractors.*

Connection of Mohr's circle with polar coordinates

When analyzing phenomena in the 12 plane, physical tensors such as the stress frequently have a matrix with respect to the orthonormal laboratory basis, $\{\mathbf{e}_1, \mathbf{e}_2, \mathbf{e}_3\}$, that is of the form

$$\begin{bmatrix} \sigma_{11} & \sigma_{12} & 0 \\ \sigma_{21} & \sigma_{22} & 0 \\ 0 & 0 & \sigma_{33} \end{bmatrix}. \quad (3.47)$$

If this represents a stress state, this structure implies that the material endures no out-of-plane shears, but it does have an out-of-plane normal stress σ_{33} . The upper 2×2 submatrix may be readily analyzed using Mohr's circle.

For cylindrical (polar) coordinates, the basis is $\{\mathbf{e}_r, \mathbf{e}_\theta, \mathbf{e}_z\}$, which is defined in terms of the orthonormal laboratory basis by

$$\mathbf{e}_r = c\mathbf{e}_1 + s\mathbf{e}_2, \quad \mathbf{e}_\theta = -s\mathbf{e}_1 + c\mathbf{e}_2, \quad \text{and} \quad \mathbf{e}_z = \mathbf{e}_3, \quad (3.48)$$

where

$$s \equiv \sin \theta \text{ and } c \equiv \cos \theta. \quad (3.49)$$

The matrix for *the same tensor* with respect to the cylindrical basis is

$$\begin{bmatrix} \sigma_{rr} & \sigma_{r\theta} & 0 \\ \sigma_{\theta r} & \sigma_{\theta\theta} & 0 \\ 0 & 0 & \sigma_{zz} \end{bmatrix}, \quad (3.50)$$

where

$$\begin{aligned} \sigma_{rr} &= c^2 \sigma_{11} + cs(\sigma_{12} + \sigma_{21}) + s^2 \sigma_{22} \\ \sigma_{\theta r} &= -cs \sigma_{11} + c^2 \sigma_{21} - s^2 \sigma_{12} + cs \sigma_{33} \\ \sigma_{\theta\theta} &= c^2 \sigma_{22} + cs(\sigma_{12} + \sigma_{21}) + s^2 \sigma_{11} \\ \sigma_{r\theta} &= -cs \sigma_{11} + c^2 \sigma_{12} - s^2 \sigma_{21} + cs \sigma_{33} \\ \sigma_{zz} &= \sigma_{33}. \end{aligned} \quad (3.51)$$

The half angle trigonometry identities state that

$$\begin{aligned} c^2 &= \frac{1}{2}[1 + \cos(2\theta)] \\ s^2 &= \frac{1}{2}[1 - \cos(2\theta)] \\ cs &= \frac{1}{2}[\sin(2\theta)]. \end{aligned} \quad (3.52)$$

Therefore the polar components of stress may be written

$$\begin{aligned} \sigma_{rr} &= \frac{\sigma_{11} + \sigma_{22}}{2} + \frac{\sigma_{11} - \sigma_{22}}{2} \cos 2\theta + \frac{\sigma_{12} + \sigma_{21}}{2} \sin 2\theta \\ \sigma_{\theta r} &= \frac{\sigma_{21} - \sigma_{12}}{2} + \frac{\sigma_{12} + \sigma_{21}}{2} \cos 2\theta + \frac{\sigma_{22} - \sigma_{11}}{2} \sin 2\theta \\ \sigma_{\theta\theta} &= \frac{\sigma_{11} + \sigma_{22}}{2} - \frac{\sigma_{11} - \sigma_{22}}{2} \cos 2\theta - \frac{\sigma_{12} + \sigma_{21}}{2} \sin 2\theta \\ \sigma_{r\theta} &= \frac{\sigma_{12} - \sigma_{21}}{2} + \frac{\sigma_{12} + \sigma_{21}}{2} \cos 2\theta + \frac{\sigma_{22} - \sigma_{11}}{2} \sin 2\theta. \end{aligned} \quad (3.53)$$

We note at this point that these equations are exactly of the form of Eqs. (4.10-4.12). In other words, expressing a tensor in terms of cylindrical coordinates is exactly the same as performing an orthogonal coordinate transformation by an angle equal to θ . Following the methods used in the appendix, we define

$$C_1 \equiv \frac{\sigma_{11} + \sigma_{22}}{2} \quad -C_2 = \frac{\sigma_{21} - \sigma_{12}}{2} \quad (3.54)$$

$$R_1^L \equiv \frac{\sigma_{11} - \sigma_{22}}{2} \quad -R_2^L = \frac{\sigma_{21} + \sigma_{12}}{2}, \quad (3.55)$$

where the superscript ‘‘L’’ stands for ‘‘Laboratory’’ to indicate that the quantity is computed using the laboratory components. * With the above substitutions, Eqs. (3.53) become

$$\begin{aligned}
 \sigma_{rr} &= C_1 + R_1^L \cos 2\theta - R_2^L \sin 2\theta \\
 \sigma_{\theta r} &= -C_2 - R_2^L \cos 2\theta - R_1^L \sin 2\theta \\
 \sigma_{\theta\theta} &= C_1 - R_1^L \cos 2\theta + R_2^L \sin 2\theta \\
 \sigma_{r\theta} &= -C_2 - R_2^L \cos 2\theta - R_1^L \sin 2\theta.
 \end{aligned} \tag{3.56}$$

Based on the structure of these equations, we introduce yet another change of variables. Specifically, let

$$R_1^L = R \cos \gamma^L \quad \text{and} \quad R_2^L = R \sin \gamma^L, \tag{3.57}$$

where the superscript “L” is used to emphasize that the value of γ^L is computed using the laboratory components, so it dictates the placement of the “ H^L ” point on Mohr’s circle corresponding to the face of the “stress” element having the normal aligned with the first laboratory base vector \mathbf{e}_1 . As shown below, the quantity R turns out to be an invariant, so it needs no “L” adornment. With the above substitution, Eqs. (3.56) become

$$\begin{aligned}
 \sigma_{rr} &= C_1 + R \cos(\gamma_L + 2\theta) \\
 \sigma_{\theta r} &= -C_2 - R \sin(\gamma_L + 2\theta) \\
 \sigma_{\theta\theta} &= C_1 - R \cos(\gamma_L + 2\theta) \\
 \sigma_{r\theta} &= -C_2 + R \sin(\gamma_L + 2\theta).
 \end{aligned} \tag{3.58}$$

This shows that the “ H^P ” point for a polar basis (corresponding to the plane whose normal is the first polar base vector \mathbf{e}_r) is located at an angle γ_P that is related to the laboratory “ H^L ” point by

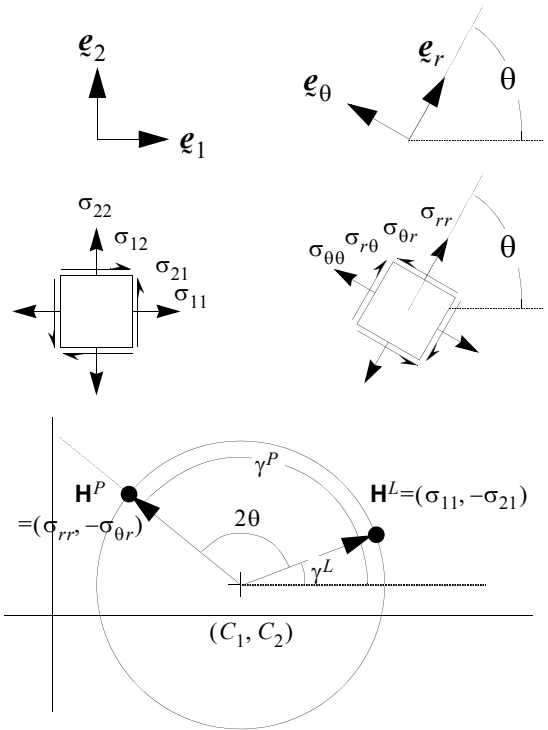
$$\gamma_P = \gamma_L + 2\theta. \tag{3.59}$$

This conclusion is occasionally expressed (especially in fracture mechanics literature) by visualizing the radial-vectors shown in the figure to be expressed via complex numbers. Thus, one could write

$$R_1^P + iR_2^P = e^{i2\theta}[R_1^L + iR_2^L], \tag{3.60}$$

where, analogously to Eq. (3.55),

$$\begin{aligned}
 R_1^P &\equiv \frac{\sigma_{rr} - \sigma_{\theta\theta}}{2} \\
 -R_2^P &= \frac{\sigma_{\theta r} + \sigma_{r\theta}}{2}.
 \end{aligned} \tag{3.61}$$



Eq. (3.60) may be written out explicitly as

* As shown below, the C_i quantities turn out to be scalar invariants and therefore give the same value regardless of the basis to which the components are referenced (so long as the basis is orthonormal). Consequently, they are not adorned with an “L” identifier.

$$\frac{\sigma_{\theta\theta} - \sigma_{rr}}{2} + i \frac{\sigma_{\theta r} + \sigma_{r\theta}}{2} = e^{i2\theta} \left[\frac{\sigma_{22} - \sigma_{11}}{2} + i \frac{\sigma_{21} + \sigma_{12}}{2} \right], \quad (3.62)$$

where we have multiplied both sides by -1 .

The in-plane part of the tensor is represented by the upper 2×2 submatrices in either the laboratory or polar basis. The in-plane part of the tensor has three invariants with respect to rotation in the plane. Specifically,

trace:

$$\frac{\sigma_{11} + \sigma_{22}}{2} = \frac{\sigma_{rr} + \sigma_{\theta\theta}}{2} = C_1 \quad (3.63)$$

determinant:

$$\sigma_{11}\sigma_{22} - \sigma_{12}\sigma_{21} = \sigma_{rr}\sigma_{\theta\theta} - \sigma_{r\theta}\sigma_{\theta r} = C_1^2 - C_2^2 - R^2 \quad (3.64)$$

magnitude:

$$\sigma_{11}^2 + \sigma_{22}^2 + \sigma_{12}^2 + \sigma_{21}^2 = \sigma_{rr}^2 + \sigma_{\theta\theta}^2 + \sigma_{r\theta}^2 + \sigma_{\theta r}^2 = C_1^2 + C_2^2 + R^2. \quad (3.65)$$

These three invariants are independent,* so the above results demonstrate that the center (C_1, C_2) and radius R of Mohr's circle are invariants — they do not change upon an in-plane change of basis.

3D Mohr's circle for 3x3 nonsymmetric matrices???

To this author's knowledge, no general theory exists for the 3D mohr's circle of nonsymmetric matrices. In the spirit of scientific inquiry, a natural first step is to explore the Mohr diagram for a variety of matrices.

In the plots that follow, the normal stress is computed in the usual way:

$$\sigma \equiv \mathbf{n} \cdot \tilde{\mathbf{F}} \cdot \mathbf{n}. \quad (3.66)$$

For the full Mohr diagram, we now redefine the “shear stress” so that it is the total magnitude of the shear stress, not just the component in the plane.

$$\tau = \sqrt{\|\tilde{\mathbf{F}} \cdot \mathbf{n}\|^2 - \sigma^2} = \sqrt{\mathbf{n} \cdot \tilde{\mathbf{F}}^T \cdot \tilde{\mathbf{F}} \cdot \mathbf{n} - \sigma^2}. \quad (3.67)$$

With this definition, $\tau > 0$ always.

We performed numerical experiments in which about 7400 points in the Mohr diagram were generated by using uniformly random unit normals.† Our hope was to educe some discernible order in the Mohr diagram. Alas, although it is apparent that order exists, we haven't the foggiest idea how to characterize it! The figure below shows dot plots on the Mohr diagram for various $[\mathbf{F}]$ matrices.

* Many people wrongly think that a 2×2 matrix corresponding to the planar part of a tensor has only two invariants. This is true for symmetric tensors, but false for nonsymmetric tensors. Consider, for example, the tensor $\alpha(\mathbf{e}_1\mathbf{e}_2)$ where α is a scalar. This tensor has a matrix with zeros everywhere except that the 12 component equals the scalar α . Both the trace and determinant of this tensor are zero, yet the tensor's magnitude, α , is nonzero and arbitrary, proving that magnitude is an independent invariant for nonsymmetric tensors.

† The document <http://me.unm.edu/~rmbrann/rotation.pdf> shows how to make uniformly random unit vectors.

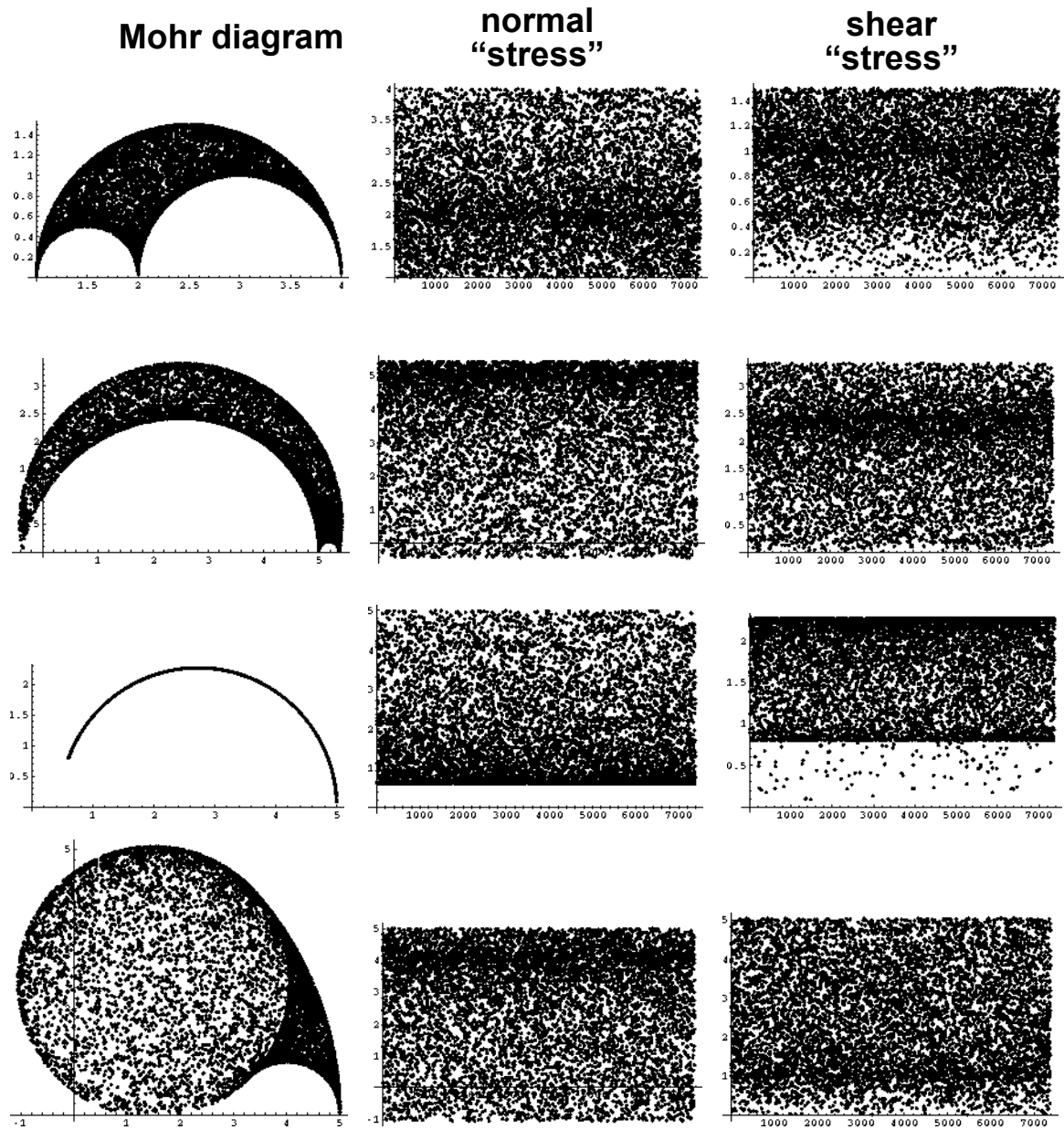


Figure 3.3. Mohr diagram for the four sample $[F]$ matrices.

$$[F] = \begin{bmatrix} 1 & 0 & 0 \\ 0 & 2 & 0 \\ 0 & 0 & 4 \end{bmatrix}, \quad [F] = \begin{bmatrix} 1 & 3 & 0 \\ 2 & 4 & 0 \\ 0 & 0 & 5 \end{bmatrix}, \quad [F] = \begin{bmatrix} 0.6 & -0.8 & 0 \\ 0.8 & 0.6 & 0 \\ 0 & 0 & 5 \end{bmatrix}, \quad \text{and } [F] = \begin{bmatrix} -1 & 2 & 0 \\ 3 & 4 & 0 \\ 0 & 0 & 5 \end{bmatrix},$$

respectively. The first matrix is symmetric. The last matrix is a generalization of the matrix in Eq. (3.35).

To explore the variety of possible results, similar plots were performed for randomly generated $[F]$ matrices. Below are two representative results when all components of $[F]$ (with respect to the lab basis) were restricted to lie in the interval $[0,1)$:

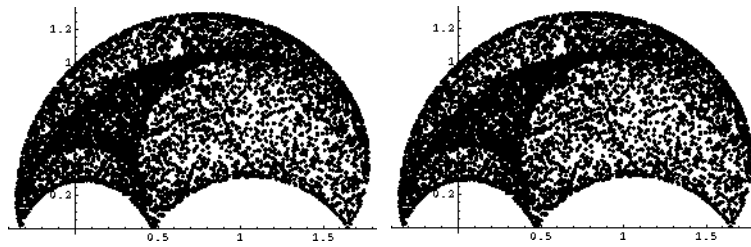


Figure 3.4. Mohr diagram for 3D matrices on $[0,1)$.

Below are further explorations in which the components of $[F]$ are uniformly random in the interval $[-1,1)$.

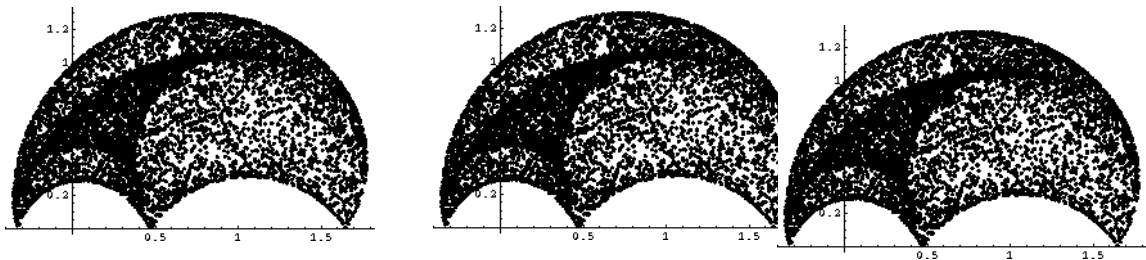


Figure 3.5. Mohr diagram for 3D matrices on $[-1,1)$

Clearly there is structure here, but its mathematical description is not obvious. Perhaps working with a different shear measure would prove useful? Suggestions would be welcomed.

4. APPENDIX

Derivation of Mohr's circle

Consider a tensor $\underline{\underline{F}}$ represented by the following matrix of components with respect to an orthonormal laboratory basis $\{\underline{\underline{E}}_1, \underline{\underline{E}}_2, \underline{\underline{E}}_3\}$:

$$\begin{bmatrix} F_{11} & F_{12} & F_{13} \\ F_{21} & F_{22} & F_{23} \\ F_{31} & F_{32} & F_{33} \end{bmatrix}. \quad (4.1)$$

In basis notation, we would write

$$\underline{\underline{F}} = F_{ij} \underline{\underline{E}}_i \underline{\underline{E}}_j. \quad (4.2)$$

We seek an expression for how the components of this tensor change upon an orthonormal change of basis. Let $\{\underline{\underline{e}}_1, \underline{\underline{e}}_2, \underline{\underline{e}}_3\}$ denote the new orthonormal basis, and let f_{ij} denote the components of $\underline{\underline{F}}$ with respect to this new basis. Then

$$\underline{\underline{F}} = f_{ij} \underline{\underline{e}}_i \underline{\underline{e}}_j. \quad (4.3)$$

The new components are found by constructing a direction cosine matrix such that

$$Q_{ij} = \underline{\underline{e}}_i \bullet \underline{\underline{E}}_j. \quad (4.4)$$

Then

$$f_{ij} = Q_{im} Q_{jn} F_{mn}, \quad (4.5)$$

or, in matrix notation,

$$\begin{bmatrix} f_{11} & f_{12} & f_{13} \\ f_{21} & f_{22} & f_{23} \\ f_{31} & f_{32} & f_{33} \end{bmatrix} = \begin{bmatrix} Q_{11} & Q_{12} & Q_{13} \\ Q_{21} & Q_{22} & Q_{23} \\ Q_{31} & Q_{32} & Q_{33} \end{bmatrix} \begin{bmatrix} F_{11} & F_{12} & F_{13} \\ F_{21} & F_{22} & F_{23} \\ F_{31} & F_{32} & F_{33} \end{bmatrix} \begin{bmatrix} Q_{11} & Q_{21} & Q_{31} \\ Q_{12} & Q_{22} & Q_{32} \\ Q_{13} & Q_{23} & Q_{33} \end{bmatrix}. \quad (4.6)$$

This calculation is tedious to perform for general basis changes, but it is relatively straightforward if the new basis shares one base vector with the lab basis.

Suppose that a new basis is constructed by rotating the lab basis by an angle θ about the $\underline{\underline{E}}_3$ axis. For this special case, the new basis is then

$$\underline{\underline{e}}_1 = \begin{Bmatrix} \cos \theta \\ \sin \theta \\ 0 \end{Bmatrix}, \quad \underline{\underline{e}}_2 = \begin{Bmatrix} -\sin \theta \\ \cos \theta \\ 0 \end{Bmatrix}, \quad \underline{\underline{e}}_3 = \begin{Bmatrix} 0 \\ 0 \\ 1 \end{Bmatrix}, \quad (4.7)$$

and the corresponding direction cosine matrix is

$$[Q] = \begin{bmatrix} \cos\theta & \sin\theta & 0 \\ -\sin\theta & \cos\theta & 0 \\ 0 & 0 & 1 \end{bmatrix}. \quad (4.8)$$

Equation (4.6), gives the new components as

$$\begin{bmatrix} f_{11} & f_{12} & f_{13} \\ f_{21} & f_{22} & f_{23} \\ f_{31} & f_{32} & f_{33} \end{bmatrix} = \begin{bmatrix} \cos\theta & \sin\theta & 0 \\ -\sin\theta & \cos\theta & 0 \\ 0 & 0 & 1 \end{bmatrix} \begin{bmatrix} F_{11} & F_{12} & F_{13} \\ F_{21} & F_{22} & F_{23} \\ F_{31} & F_{32} & F_{33} \end{bmatrix} \begin{bmatrix} \cos\theta & -\sin\theta & 0 \\ \sin\theta & \cos\theta & 0 \\ 0 & 0 & 1 \end{bmatrix} \quad (4.9)$$

Multiplying this out gives

$$\begin{aligned} f_{11} &= \frac{F_{11} + F_{22}}{2} + \frac{F_{11} - F_{22}}{2} \cos 2\theta + \frac{F_{12} + F_{21}}{2} \sin 2\theta \\ f_{21} &= \frac{F_{21} - F_{12}}{2} + \frac{F_{12} + F_{21}}{2} \cos 2\theta + \frac{F_{22} - F_{11}}{2} \sin 2\theta \\ f_{31} &= F_{31} \cos \theta + F_{32} \sin \theta \end{aligned} \quad (4.10)$$

$$\begin{aligned} f_{22} &= \frac{F_{11} + F_{22}}{2} - \frac{F_{11} - F_{22}}{2} \cos 2\theta - \frac{F_{12} + F_{21}}{2} \sin 2\theta \\ f_{12} &= \frac{F_{12} - F_{21}}{2} + \frac{F_{12} + F_{21}}{2} \cos 2\theta + \frac{F_{22} - F_{11}}{2} \sin 2\theta \\ f_{32} &= F_{32} \cos \theta + F_{31} \sin \theta \end{aligned} \quad (4.11)$$

$$\begin{aligned} f_{33} &= F_{33} \\ f_{23} &= F_{23} \cos \theta - F_{13} \sin \theta \\ f_{13} &= F_{13} \cos \theta + F_{23} \sin \theta. \end{aligned} \quad (4.12)$$

Observe:

- The formulas for the f_{11} , f_{22} , f_{12} , and f_{21} components are independent of the F_{i3} and F_{3j} components. In other words, the upper-left 2×2 submatrix of $[f]$ depends only on the upper-left 2×2 submatrix of $[F]$ and the rotation angle. Henceforth, we are interested primarily in this submatrix.
- The formula for f_{22} can be obtained from the formula for f_{11} by replacing θ by $\theta + \frac{\pi}{2}$.
- The formula for f_{12} can be obtained from the formula for f_{21} by replacing θ by $\theta + \frac{\pi}{2}$, and then multiplying the result by -1 .

The last two observations (and a similar statement for the out of plane components, f_{31} and f_{13}) follow intuitively if we “pretend” that the $[F]$ matrix is a stress, as sketched in Fig. 4.1. Specifically, if we had instead used a \mathbf{e}_i^* basis that was rotated 90° farther than the \mathbf{e}_i basis, then f_{11}^* with respect to the \mathbf{e}_i^* basis would have to equal the f_{22} from the original rotated basis.

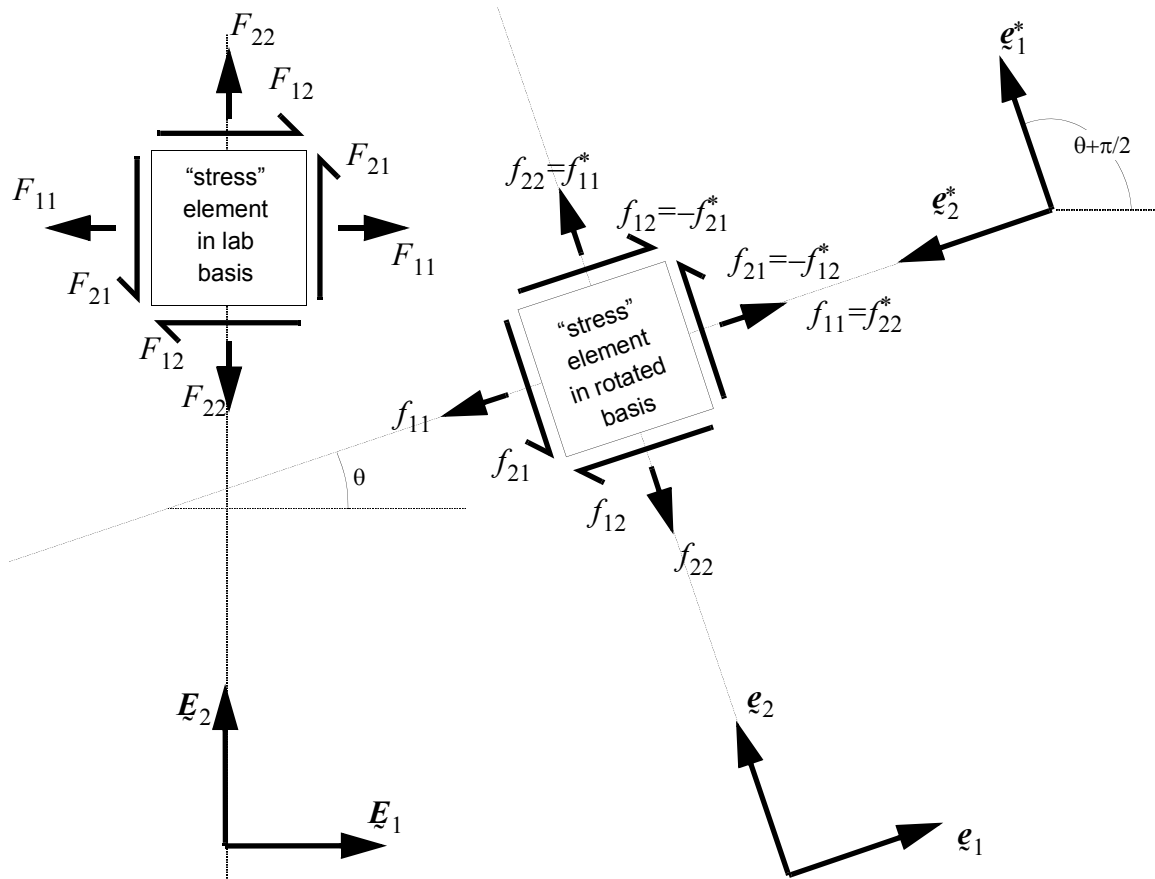


Figure 4.1. The same “stress” element as seen by two different observers. Note that the 11 component with respect to the “star” basis is equal to the 22 component with respect to the unstarred basis.

Recall that the “stresses” f_{22} and f_{12} , on the face whose outward normal is \mathbf{e}_2 can be obtained by using the formulas for f_{11} and f_{21} with the angle replaced by $\theta + \pi/2$. The shear component f_{12} also changes sign.

We now denote the normal “stress” acting on the 1-face by $\sigma \equiv f_{11}$. The two shear “stresses” acting on this face will be defined $\tau \equiv -f_{21}$ and $s \equiv f_{31}$. These are the three components of the “traction” acting on the face of the stress element whose normal is aligned with \mathbf{e}_1 . For reasons explained later, the shear stress has been defined as the *negative* of f_{21} . This shear will be called positive if it tends to rotate the stress element in the *clockwise* direction. Hence, referring to Eq. (4.10), we note

$$\sigma(\theta) = \frac{F_{11} + F_{22}}{2} + \frac{F_{11} - F_{22}}{2} \cos 2\theta + \frac{F_{12} + F_{21}}{2} \sin 2\theta \quad (4.13)$$

$$\tau(\theta) = -\left(\frac{F_{21} - F_{12}}{2} + \frac{F_{12} + F_{21}}{2} \cos 2\theta + \frac{F_{22} - F_{11}}{2} \sin 2\theta \right). \quad (4.14)$$

$$s(\theta) = F_{31} \cos \theta + F_{32} \sin \theta \quad (4.15)$$

Naturally, it is wise to verify that these formulas give the correct results when the local basis happens to be aligned with the lab basis (*i.e.*, when $\theta=0$). Namely, the normal and shear stresses correspond to those on the \underline{E}_1 face:

$$\sigma(0) = F_{11} \quad \text{and} \quad \tau(0) = -F_{21} \quad \text{and} \quad s(0) = F_{31} \quad (4.16)$$

Similarly, when the local basis differs from the lab basis by $\theta=\pi/2$ then the normal and shear stresses correspond to those on the \underline{E}_2 face:

$$\sigma(\pi/2) = F_{22} \quad \text{and} \quad \tau(\pi/2) = F_{12} \quad \text{and} \quad s(\pi/2) = F_{32} \quad (4.17)$$

In general, as the orientation of the face varies, σ , τ , and s vary with the orientation angle θ and may be plotted parametrically against each other. We will now demonstrate that this parametric curve in σ vs. τ space turns out to be a circle. We will furthermore show that the points defined by Eqs. (4.16) and (4.17) turn out to be diametrically opposite each other on the circle.

Looking closely at Eqs. (4.13) and (4.14), we see that F_{11} and F_{22} appear in pairs, either summed or subtracted. Similarly, the shear components F_{12} and F_{21} appear either summed or subtracted. This motivates the following change of variables. Let

$$C_1 \equiv \frac{F_{11} + F_{22}}{2} \quad -C_2 = \frac{F_{21} - F_{12}}{2} \quad (4.18)$$

$$R_1 \equiv \frac{F_{11} - F_{22}}{2} \quad -R_2 = \frac{F_{21} + F_{12}}{2}. \quad (4.19)$$

Then Eqs. (4.13) and (4.14) become

$$\sigma(\theta) = C_1 + R_1 \cos 2\theta - R_2 \sin 2\theta \quad (4.20)$$

$$\tau(\theta) = C_2 + R_2 \cos 2\theta + R_1 \sin 2\theta. \quad (4.21)$$

Looking at the structure of this result motivates an extension in our change of variables. Namely, introduce two variables R and γ such that

$$R_1 = R \cos \gamma \quad \text{and} \quad R_2 = R \sin \gamma \quad (4.22)$$

Then

$$\sigma(\theta) = C_1 + R \cos(\gamma + 2\theta) \quad (4.1a)$$

$$\tau(\theta) = C_2 + R \sin(\gamma + 2\theta). \quad (4.1b)$$

Note that $(\sigma - C_1)^2 + (\tau - C_2)^2 = R^2$. Thus the curve which is parametrically defined by $\sigma(\theta)$ and $\tau(\theta)$ is in fact a circle — Mohr's circle — centered at the point (C_1, C_2) in the σ - τ plane.

Now consider two planes whose orientations are θ^* and $\theta^* + \pi/2$. In other words, they differ by 90° in the physical plane. Then Eq. (4.1) shows that the corresponding points on Mohr's circle must be diametrically opposite each other. Thus, the two points of Eqs. (4.16) and (4.17), uniquely define the Mohr's circle. The "H-plane" of Eq. (4.16) corresponds to $\theta=0$. The "V-plane" of Eq. (4.17) corresponds to $\theta=\pi/2$.

Referring to Eq. (4.1) we see that a plane that differs from the H-plane by an angle θ measured counterclockwise in physical space will correspond to a point on Mohr's circle that is located at an angle 2θ measured counterclockwise from the H-point on Mohr's circle.

Recall Eq. (4.15) for the out-of-plane shear stress:

$$s(\theta) = F_{31} \cos \theta + F_{32} \sin \theta \quad (4.1)$$

This formula may be written more compactly as

$$s(\theta) = \sqrt{F_{31}^2 + F_{32}^2} \sin(\theta - \theta^*) \quad (4.2)$$

where θ^* is the angle at which $s = 0$.

$$\text{Namely, } \cos \theta^* = \frac{F_{32}}{\sqrt{F_{31}^2 + F_{32}^2}} \text{ and } \sin \theta^* = \frac{-F_{31}}{\sqrt{F_{31}^2 + F_{32}^2}} \quad (4.3)$$

This result shows that the out-of-plane shear varies sinusoidally.

Polar decomposition in 2-D

Consider a matrix of the following form

$$\begin{bmatrix} F_{11} & F_{12} & 0 \\ F_{21} & F_{22} & 0 \\ 0 & 0 & F_{33} \end{bmatrix} \quad \text{with} \quad F_{33} > 0 \quad \text{and} \quad \det[F] > 0. \quad (4.4)$$

If the matrix $[F]$ is invertible, the polar decomposition theorem states that it permits a decomposition of the form $F = VR$ for which R is orthogonal and V is both symmetric and positive definite.

For the decomposition to be unique, positive definiteness of U and V are *requirements*, not consequences. In what follows, we serendipitously produce suitable R and V matrices and invoke uniqueness to claim that they are the only solutions. By serendipity, we claim that

$$[R] = \begin{bmatrix} \cos\beta & -\sin\beta & 0 \\ \sin\beta & \cos\beta & 0 \\ 0 & 0 & 1 \end{bmatrix}, \quad (4.5)$$

where

$$\cos\beta = \frac{F_{11} + F_{22}}{\sqrt{(F_{11} - F_{22})^2 + (F_{21} - F_{12})^2}} \quad \text{and} \quad (4.6)$$

$$\sin\beta = \frac{F_{21} - F_{12}}{\sqrt{(F_{11} - F_{22})^2 + (F_{21} - F_{12})^2}}. \quad (4.7)$$

The positive square root is to be taken. Observe that we do *not* define $\beta = \text{atan}\left(\frac{F_{21} - F_{12}}{F_{11} + F_{22}}\right)$.

Such a definition is not unique because the arc-tangent has two solutions in the interval from 0 to 2π . In numerical applications, the two-argument arc-tangent may be used.

Note that $[R][R]^T = [I]$ and therefore $[R]$ is orthogonal as required. The stretch $[V]$ is obtained by $[V] = [F][R]^T$. It is a straightforward (but tedious) exercise to then prove that $[V]$ is both symmetric and positive definite, thereby proving that Eq. (4.5) does indeed represent the unique polar rotation matrix. Symmetry of $[V]$ is fairly simple to prove, but keep in mind that verifying symmetry is not enough! Positive definiteness must be proved by demonstrating that $V_{11} > 0$ and $V_{11}V_{22} - V_{12}V_{21} > 0$ and $\det[V] > 0$. The last inequality is trivial to prove because, by construction, $\det[V] = \det[F]\det[R]^T = \det[F]$, which is positive by premise. The second inequality is equally easy due to the partitioned structure of the $[F]$. The first inequality ($V_{11} > 0$) follows by invoking the fact that $F_{11}F_{22} - F_{12}F_{21} > 0$.

Connection to Mohr's circle. Substituting Eq. (4.18) into (4.6) and (4.7) gives

$$\cos\beta = \frac{C_1}{\sqrt{C_1^2 + C_2^2}} \quad \text{and} \quad \sin\beta = \frac{-C_2}{\sqrt{C_1^2 + C_2^2}}. \quad (4.8)$$

Thus, the angle that the center of Mohr's circle makes with the σ -axis is equal to $-\beta$.

DRAFT
Rebecca Brannon

October 29, 2003 6:19 pm
APPENDIX